ASD TECHNICAL REPORT 61-118

UNIFIED ANALYSIS OF LINEAR FEEDBACK SYSTEMS

DUANE T. McRUER

SYSTEMS TECHNOLOGY, INC.

JULY 1961

AERONAUTICAL SYSTEMS DIVISION

ASD TECHNICAL REPORT 61-118

UNIFIED ANALYSIS OF LINEAR FEEDBACK SYSTEMS

DUANE T. McRUER

SYSTEMS TECHNOLOGY, INC.

JULY 1961

FLIGHT CONTROL LABORATORY
CONTRACT No. AF 33(616)-5961
PROJECT No. 8219
TASK No. 82162

AERONAUTICAL SYSTEMS DIVISION
AIR FORCE SYSTEMS COMMAND
UNITED STATES AIR FORCE
WRIGHT-PATTERSON AIR FORCE BASE, OHIO

McGregor & Werner, Inc., Dayton, O.
900 - November 1961 - 10-332 & 333

FOREWORD

This report represents one phase of an analytical investigation which, overall, is aimed at the determination of generalized dynamic requirements for advanced vehicle flight control systems in terms of weapon system characteristics or of the factors which generate these characteristics. The fundamental analytical tools used throughout this investigation have included a composite of servo analysis techniques — some well known, some obscure, and some new — which have been integrated into a so-called "Unified Servo Analysis Method." Since a knowledge of this unified method is necessary to follow many of the developments in other documents in the series, this report has been prepared to provide a summary of the integrated techniques and to serve as a basic reference.

The research reported here was sponsored by the Flight Control Laboratory, Aeronautical Systems Division, Air Force Systems Command, as part of Project No. 8219, Task No. 82162. It was conducted at Systems Technology, Inc., under Contract AF 33(616)-5961. The ASD project engineers have been Mr. George Xenakis and Mr. Ronald O. Anderson.

The author has been materially assisted by Mr. J. D. McDonnell, who performed many of the illustrative calculations; by Messrs. I. L. Ashkenas and D. Graham, who have made several helpful suggestions; and by Mr. J. Taira, who prepared much of the report for publication. Special acknowledgment is due Mr. R. J. Wasicko for his efforts in thoroughly reviewing and checking a draft of the report, and for his many constructive suggestions on organization and content.

ABSTRACT

A summary is given of techniques and concepts useful in the analysis of linear feedback systems; these procedures are then correlated and integrated into a unified analysis method. The central feedback system analysis problem discussed is that of finding complete closed-loop system characteristics from a knowledge of the open-loop transfer function. Several forms of graphical representation for open-loop transfer functions, including pole-zero plots and generalized G(s) logarithmic diagrams, are considered. The use of these graphical forms in generalized root-locus and decomposition techniques to find closed-loop transfer functions is illustrated with examples. The various feedback system analysis procedures are shown to have a common theoretical connection and to be supplementary techniques when used in an integrated manner to attack specific problems.

PUBLICATION REVIEW

This report has been reviewed and is approved.

FOR THE COMMANDER:

Charles B. Westbrook

CHARLES B. WESTBROOK
Chief, Aerospace Mechanics Branch
Flight Control Laboratory

TABLE OF CONTENTS

Section		Page
I	INTRODUCTION	1
II	DIRECTLY AVAILABLE CLOSED-LOOP DATA	5
III	SUMMARY OF ROOT-LOCUS TECHNIQUE.	11
	A. General Principles.	11
	B. Properties of the Locus	14
IV	THE LOGARITHMIC G(s) METHODS.	21
	A. General	21
	B. Properties of Continuous G(s) Bode Plots	23
	C. Calculation of Closed-Loop Roots Using G(s) Bode Plots. .	33
	D. Calculation of Closed-Loop Roots by Decomposition . . .	47
V	CONNECTIONS BETWEEN THE METHODS.	53
REFERENCES		62

LIST OF ILLUSTRATIONS

Figure		Page
1	Single Loop Linear Feedback System	1
2	Vector Plots for Typical Factors of G(s)	12
3	Angle Measurement Procedure in Root Locus Construction	12
4	Illustrative Root Locus Departure Angles	16
5	Illustrative Root Locus for $G(s) = \frac{K}{s(s+a)(s+b)}$	18
6	Root Loci for Simple Systems	19-20
7	s-Plane Loci for Various Special Values of s	22
8	Elementary Properties of the First Order Pole $G(\lambda) = \frac{1}{\lambda + 1}$	24
9	Elementary Properties of the Second Order Pole $G(\lambda) = \frac{1}{\lambda^2 + 2\zeta\lambda + 1}$	26
10	High Frequency Phase Asymptotes of $G(\lambda) = \frac{1}{\lambda + 1}$, $G(\lambda) = \frac{1}{\lambda^2 + 2\zeta\lambda + 1}$	32
11	Phase Break Frequencies of $G(\lambda) = \frac{1}{\lambda + 1}$, $G(\lambda) = \frac{1}{\lambda^2 + 2\zeta\lambda + 1}$	34
12	Departures from Asymptotes of $G(\lambda) = \frac{1}{\lambda + 1}$	35
13a	Departures from Asymptotes of $G(\lambda) = \frac{1}{\lambda^2 + 2\zeta\lambda + 1}$, $\zeta = 0$	36
13b	Departures from Asymptotes of $G(\lambda) = \frac{1}{\lambda^2 + 2\zeta\lambda + 1}$, $\zeta = -0.2$	37
13c	Departures from Asymptotes of $G(\lambda) = \frac{1}{\lambda^2 + 2\zeta\lambda + 1}$, $\zeta = -0.4$	38
13d	Departures from Asymptotes of $G(\lambda) = \frac{1}{\lambda^2 + 2\zeta\lambda + 1}$, $\zeta = -0.6$	39
13e	Departures from Asymptotes of $G(\lambda) = \frac{1}{\lambda^2 + 2\zeta\lambda + 1}$, $\zeta = -0.8$	40
13f	Departures from Asymptotes of $G(\lambda) = \frac{1}{\lambda^2 + 2\zeta\lambda + 1}$, $\zeta = \pm 1.0$	41
13g	Departures from Asymptotes of $G(\lambda) = \frac{1}{\lambda^2 + 2\zeta\lambda + 1}$, $\zeta = 0.5$	42

Figure		Page
14	Logarithmic Plots of $G(s) = \frac{K}{s(s+1)(\frac{s}{5}+1)}$	44
15	Locus of Closed-Loop Transfer Function Inverse Time Constants and Undamped Natural Frequency for $G(s) = \frac{K}{s(s+1)(\frac{s}{5}+1)}$	45
16	Establishment of Asymptotic Plot for Closed-Loop System for $G(s) = \frac{K}{s(\frac{s}{a}+1)(\frac{s}{b}+1)}$	46
17	Determination of Closed-Loop Parameters with the Aid of the Nichols Chart.	48
18	Determination of ζ from Amplitude Ratio Peak	50
19	Frequency at Which AR_{MAX} Occurs.	51
20	Potential Surveys Along Various Lines in the s-Plane.	55
21	Lines of Constant Phase, or Phase Angle Loci for $G(s) = \frac{K}{s(s+1)(s+5)}$	56
22	Three-Dimensional Model of the Various Graphical Forms for G(s) and the Three-Dimensional Root Locus	57
23	Solution for Closed-Loop Roots for $G(s) = \frac{4[(\frac{s}{7.5})^2 + \frac{2(0.1)s}{7.5} + 1]}{s[(\frac{s}{10})^2 + \frac{2(0.1)s}{10} + 1][(\frac{s}{15})^2 + \frac{2(0.1)s}{15} + 1]}$	58
24	High Frequency Portion of Root Locus for $G(s) = \frac{1600[s^2 + 2(0.1)(7.5)s + (7.5)^2]}{s[s^2 + 2(0.1)(10)s + (10)^2][s^2 + 2(0.1)(15)s + (15)^2]}$	60

LIST OF SYMBOLS

a	Polynomial coefficient.
a	Open-loop pole location.
A(s)	Numerator of open-loop transfer function (polynomial in s); A(0) = 1.
AR	Amplitude ratio.
b	Polynomial coefficient.
b	Open-loop pole location.
B(s)	Denominator of open-loop transfer function (polynomial in s); B(0) = 1.
C(s)	Transform of system output.
db	Decibel.
E(s)	Transform of error signal.
G(s)	Open-loop transfer function.
$G_{rc}(s)$	Closed-loop transfer function relating output to input.
$G_{re}(s)$	Closed-loop transfer function relating error to input.
i	Current.
j	$\sqrt{-1}$.
K	Open-loop gain; the frequency invariant portion of the open-loop transfer function.
M_p	Peak overshoot of the system frequency response.
p	Open-loop poles.
r_D	Magnitude of the vector from the open-loop pole to the point s.
r_N	Magnitude of the vector from the open-loop zero to the point s.
s	Laplace transform variable, $s = \sigma + j\omega$.
T	First order time constant.
u	Normalized running variable along constant ξ for $G(\lambda)$ transfer function; $u = \lvert\lambda\rvert$.
U	Real part of the open-loop transfer function.
V	Imaginary part of the open-loop transfer function.

z	Open-loop zeros.
$\alpha(s)$	Numerator of open-loop transfer function (polynomial in s); highest order term has coefficient of unity.
$\beta(s)$	Denominator of open-loop transfer function (polynomial in s); highest order term has coefficient of unity.
γ	Angle associated with root locus departure angle.
ζ	Damping ratio of linear second-order system; particularized by the subscript.
θ	Constant phase angle.
κ	Root-locus gain constant.
λ	Nondimensionalized variable for normalized first and second order factors defined by $s = \lambda/T$ and $s = \omega_n\lambda$, respectively.
μ	Running variable along constant ξ for G(s) transfer function; $u = \|s\|$.
ξ	The negative of the damping ratio for a special value of s; $\xi = \frac{\sigma_1}{\sqrt{\sigma_1^2 + \omega_1^2}}$
σ	The real portion of the complex variable $s = \sigma + j\omega$.
σ_A	Point of intersection on the real axis of linear asymptotes of root locus.
τ	Time constant.
φ_A	Angle made by the asymptote of root locus and real axis.
φ_D	Phase angle contribution of the denominator terms (open-loop poles); particularized by the subscript.
φ_N	Phase angle contribution of the numerator terms (open-loop zeros); particularized by the subscript.
$\varphi(s)$	Phase angle of the open-loop transfer function.
Φ	Potential.
ω	Frequency; $j\omega$ is the imaginary portion of the complex variable $s = \sigma + j\omega$.
ω	Undamped natural frequency of a second order mode; particularized by the subscript.
ω_p	Frequency at which peak overshoot of the system frequency response occurs.

Special Subscripts

A	Asymptote.
c	Closed-loop quantities.
CL	Closed loop.
D	Denominator.
db	Decibel.
MAX	Maximum.
N	Numerator.
o	Point of reference.
p	Peak.

Mathematical Symbols

Σ	Summation.
Π	Product.
$\lvert\ \rvert$	Magnitude or absolute value.
$\gg$	Much greater than.
$\ll$	Much less than.
$\leq$	Less than or equal to.
$\geq$	Greater than or equal to.
$\angle$	Phase angle.
$\neq$	Not equal to.
∇	"Del" or the gradient operator.
$\propto$	Proportional to.
∂	Partial derivative.

SECTION I

INTRODUCTION

In general the analysis of systems which contain feedback elements involves the determination of system closed-loop behavior from a knowledge of open-loop and input signal properties. When a set of linear constant-coefficient differential equations can be used to describe system operations, the system and element characteristics can be specified completely by a series of transfer functions. The properties of input signals do not interact with those of the various transfer functions, so the system possesses an "independent identity."

Ordinarily transfer functions of system elements are easily developed by direct consideration of the elements, while the determination of closed-loop system characteristics is more difficult. Accordingly, for system analysis the major activity is to glean information about closed-loop transfer functions from known open-loop characteristics. In the context of the single loop system of Fig. 1, the fundamental linear feedback system analysis problem can be stated as: given the open-loop transfer function $G(s)$, obtain information about the closed-loop transfer functions $C(s)/R(s)$ and $E(s)/R(s)$. Since the performance of the closed-loop system in terms of stability, accuracy, and speed of response can largely be inferred from the closed-loop transfer function, the methods and techniques used to solve this restricted system analysis problem have long been central to feedback system studies.

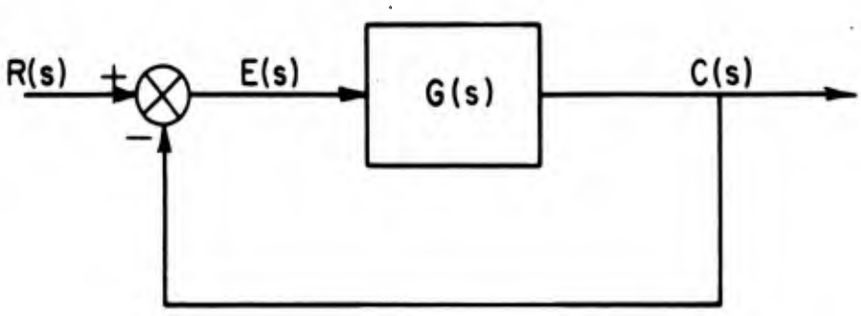

$$\frac{C(s)}{R(s)} = \frac{G(s)}{1+G(s)}$$

$$\frac{E(s)}{R(s)} = \frac{1}{1+G(s)}$$

Fig. 1. Single Loop Linear Feedback System

Manuscript released by the author November 1960; revised manuscript released for publication as an ASD Technical Report February 1961.

Historically the attack on the linear feedback system analysis problem has proceeded along two artificially separated lines—commonly referred to as "frequency response" and "root locus." Each of these approaches has attained a high degree of autonomous maturity, yet this very fact has tended to exaggerate a segregation of methods which fundamentally have much to offer as complementary techniques. This report takes an eclectic view of available methods which emphasizes their close ties and supplementary character. The primary intent is to combine the various methods into a "unified" technique which is more efficient and flexible than any one method alone.

In general, the open-loop transfer function $G(s)$ is a ratio of rational polynomials in the Laplace transform complex variable, s, so the totality of knowledge about $G(s)$ or the closed-loop transfer functions are their gains, poles, and zeros.* Thus, in principle the system analysis problem is simply that of factoring higher order algebraic equations. Such an apparently straightforward procedure, using conventional methods, unfortunately requires effort of herculean proportions when complex systems are considered. The application of modern computing machinery alleviates this problem, but this approach gives little insight into the interrelationships which exist between open- and closed-loop parameters. Consequently for the last three decades a great deal of technical activity and effort has been devoted to the development of methods which start with the open-loop $G(s)$ and provide information about the closed-loop $1 + G(s)$ [or $G/(1 + G)$ and $1/(1 + G)$]. Almost all of these techniques are specialized operations upon graphical representations of $G(s)$ to provide knowledge about the factors of $1 + G(s)$. The degree to which the closed-loop unknowns are revealed by the several methods varies from a mere assurance that no zeros of $1 + G(s)$ appear in particular portions of the s-plane (References 1-4), to exact and detailed knowledge of all the factors. The chief interest here shall be in methods which yield information of the latter variety; accordingly the statement of the linear feedback system analysis problem shall be further limited to: given $G(s)$, find the poles and zeros of the closed-loop quantities $1 + G(s)$, $(1 + G)^{-1}$, or $G/(1 + G)$.

Within the frame of reference to be used the open-loop transfer function $G(s)$ is known in analytical form, and can also be represented graphically in two basic ways: (1) as a plot of discrete points denoting the singularities (poles and zeros) of $G(s)$, or (2) as a continuous plot of some function of $G(s)$ versus some function of either $s = \sigma + j\omega$, or specialized values of s such as $s = j\omega$ or $s = \pm\sigma$. All three forms, the analytical and both graphical representations, implicitly contain sufficient information to specify completely poles and zeros of the closed-loop transfer functions $G/(1 + G)$ or $1/(1 + G)$—the trick is to make the implicit potentialities explicit realities. In the

---

*For simplicity, only single unity feedback loop systems, such as that in Fig. 1, shall be considered. This restriction does not result in significant loss of generality since any linear feedback system, regardless of its complexity, can be put into a form where the system element transfer blocks are either multiplying one another or are involved in operations like $(1 + G)^{\pm 1}$ or $G/(1 + G)$, etc., perhaps repetitively. The restriction to a rational form of $G(s)$ does result in loss of generality, although all the methods to be discussed are easily extended to cover transfer functions which include such terms as $e^{-\tau s}$.

following treatment major attention shall be devoted to procedures using the graphical representations. While, in practice, the methods derived from the two basic forms of plots are best used as different aspects of one unified technique of analysis, they shall be summarized here as more or less distinct methods to simplify the explanation, and subsequently related. Thus, the report will have four primary sections, viz: (1) a review of closed-loop information directly and readily obtained from G(s); (2) a short summary of the distinctive features of the root-locus method; (3) a somewhat more extended discussion of the elements and operations involved in the logarithmic G(s) methods; and (4) a discussion which emphasizes the essential theoretical unity of the individual methods and, with the aid of examples, illustrates their complementary character.

SECTION II

DIRECTLY AVAILABLE CLOSED-LOOP DATA

The open-loop transfer functions of interest here possess the general form

$$G(s) = \frac{C(s)}{E(s)} = K \frac{s^n + a_1 s^{n-1} + a_2 s^{n-2} + \cdots a_n}{s^{m+n} + b_1 s^{m+n-1} + b_2 s^{m+n-2} + \cdots b_{m+n}} = K \frac{\sum_{j=0}^{n} a_j s^{n-j}}{\sum_{i=0}^{m+n} b_i s^{m+n-i}}$$

$$= K \frac{\alpha(s)}{\beta(s)} = K \frac{\prod_{j=1}^{n} (s + z_j)}{\prod_{i=1}^{m+n} (s + p_i)} \tag{1}$$

where the a's, b's, and K are real, the open-loop zeros and poles ($-z_j$ and $-p_i$) can be either real or complex in conjugate pairs, and $m \geq 1$. The two closed-loop direct transfer functions of interest are those relating output and error to input.

Output/Input Transfer Function:

$$G_{rc}(s) = \frac{C(s)}{R(s)} = \frac{G(s)}{1 + G(s)} = \frac{K\alpha(s)}{\beta(s) + K\alpha(s)} \tag{2}$$

Error/Input Transfer Function:

$$G_{re}(s) = \frac{E(s)}{R(s)} = \frac{1}{1 + G(s)} = \frac{\beta(s)}{\beta(s) + K\alpha(s)} \tag{3}$$

From Eq. (1) and (2) it is apparent that the zeros of G(s) and those of the output/input transfer function $G_{rc}(s)$ are identical; and that the zeros of the error/input transfer function $G_{re}(s)$ are the poles of G(s). Since $\alpha(s)$ and $\beta(s)$ are known a priori, the determination of the zeros of $1 + G(s)$ or $\beta(s) + K\alpha(s)$ constitutes the entire analysis problem.

The theory of equations provides some rules which are of occasional use in this problem. Consider the closed-loop transfer function $G_{rc}(s)$, which, using the subscript c to indicate closed-loop quantities, becomes

$$G_{rc}(s) = \frac{K\alpha(s)}{\beta(s) + K\alpha(s)} = \frac{K(s^n + a_1 s^{n-1} + \cdots + a_n)}{s^{m+n} + b_1 s^{m+n-1} \cdots + (b_m + K)s^n + \cdots + (b_{m+n} + Ka_n)}$$

$$= \frac{K(s^n + a_1 s^{n-1} + \cdots + a_n)}{\prod_{i=1}^{q} (s^2 + 2\zeta_{c_i}\omega_{c_i} s + \omega_{c_i}^2) \prod_{i=2q}^{m+n} (s + p_{c_i})} \tag{4}$$

In Eq. (4) all the complex conjugate closed-loop factors are joined to form q quadratics, each characterized by an undamped natural frequency ω_{c_i} and a damping ratio ζ_{c_i}; and the remaining n+m - 2q closed-loop poles, $-p_{c_i}$, are real. For a polynomial with unity coefficient in its first (highest order) term, the negative of the sum of the roots is the coefficient of the second term, the sum of the products of roots taken two at a time is the third term, etc., and the product of the negatives of the roots is the constant term. Consequently when the open-loop transfer function is such that $m \geq 2$, the sum of the open-loop and closed-loop poles will have the same value, since the open-loop transfer function numerator has no effect on the second coefficient of the denominator polynomial of the closed-loop transfer function. Thus,

$$\sum_{i=1}^{q} 2\zeta_{c_i}\omega_{c_i} + \sum_{i=2q}^{m+n} p_{c_i} = b_1 \; ; \; m \geq 2 \tag{5}$$

If $m = 1$, b_1 is replaced by $b_1 + \kappa$, and

$$\sum_{i=1}^{q} 2\zeta_{c_i}\omega_{c_i} + \sum_{i=2q}^{m+n} p_{c_i} = b_1 + \kappa \; ; \; m = 1 \tag{6}$$

Most of the other relations from the theory of equations are not particularly useful, although the product of the negatives of the roots relation,

$$\prod_{i=1}^{q} \omega_{c_i}^2 \prod_{i=2q}^{m+n} p_{c_i} = b_{m+n} + \kappa a_n \tag{7}$$

is occasionally of value, especially in those systems where either b_{m+n} or a_n is zero.

A variety of useful approximations for closed-loop poles can be found by considering regions of s where the magnitude of the open-loop transfer function, $|G(s)|$, is either much greater than, much less than, or near unity. These regions can be set up in terms of special values for s, such as $s = j\omega$, without any loss of essential information. The various regions are then:

1. "Large" Amplitude Ratio – values of ω where $|G(j\omega)| \gg 1$
2. "Crossover" Region – values of ω where $|G(j\omega)|$ is near unity
3. "Small" Amplitude Ratio – values of ω where $|G(j\omega)| \ll 1$

The boundaries between regions are not sharp lines of demarcation, although values of $|G(j\omega)| \geq 10$ and $|G(j\omega)| \leq 1/10$ can be considered well within the "large" and "small" amplitude ratio regions, respectively.*

Limiting conditions as $|G(j\omega)|$ becomes much greater or less than unity leads to Table I. As a consequence, approximate values for certain of the closed-loop poles are:

1. the open-loop zeros occurring in the regions of $s = j\omega$ where $|G(j\omega)|$ is much greater than unity; and

2. the open-loop poles which are within the regions of $s = j\omega$ where $|G(j\omega)|$ is much smaller than unity.

Table I

Closed-Loop Poles for Large and Small Values of $G(j\omega)$

Closed-Loop Quantity	Exact Relationship	Approximations	
		$\|G(j\omega)\| \gg 1$	$\|G(j\omega)\| \ll 1$
$\|G_{rc}(j\omega)\| = \left\|\frac{G(j\omega)}{1 + G(j\omega)}\right\|$	$\left\|\frac{\kappa\alpha(j\omega)}{\beta(j\omega) + \kappa\alpha(j\omega)}\right\|$	1	$\kappa\left\|\frac{\alpha(j\omega)}{\beta(j\omega)}\right\|$
$\|G_{re}(j\omega)\| = \left\|\frac{1}{1 + G(j\omega)}\right\|$	$\left\|\frac{\beta(j\omega)}{\beta(j\omega) + \kappa\alpha(j\omega)}\right\|$	$\frac{1}{\kappa}\left\|\frac{\beta(j\omega)}{\alpha(j\omega)}\right\|$	1

For most practical linear feedback systems either the condition $|G(j\omega)| \gg 1$ or $|G(j\omega)| \ll 1$ obtains over large ranges in $s = j\omega$, so approximations to the closed-loop poles occurring within these ranges are essentially known a priori from the values of the open-loop poles and zeros also contained in the same regions of s.

The simple considerations given above hardly constitute a complete answer to the analysis problem, but they do provide the basis for extremely rapid approximate solutions in some cases. For example, consider the open-loop transfer function

$$G(j\omega) = \frac{2 \cdot 10^5 (j\omega + 1)}{(j\omega)^2 (j\omega + 100)(j\omega + 200)}$$

---

*In terms of the $G(j\omega)$ Bode plots considered later, these same considerations correspond to $20 \log |G(j\omega)| \geq 20$ db for "large" amplitude ratio $20 \log |G(j\omega)| \leq -20$ db for "small" amplitude ratio.

Table II

Open- and Closed-Loop Transfer Functions for Elementary Systems

	Open-Loop Forms G(s)	Closed-Loop Form G(s)/[1 + G(s)]
①	K	$\frac{K}{K+1}$
②	$\frac{K}{s}$	$\frac{K}{s+K}$
③	$\frac{K}{s+p}$	$\frac{K}{s+(p+K)}$
④	$\frac{K(s+z)}{s+p}$	$\frac{K}{K+1}\left[\frac{s+z}{s+\frac{p+Kz}{K+1}}\right]$
⑤	$\frac{K}{s(s+p)}$	$\frac{K}{s^2+ps+K}$
⑥	$\frac{K(s+z)}{s(s+p)}$	$\frac{K(s+z)}{s^2+(p+K)s+Kz}$
⑦	$\frac{K}{(s+p_1)(s+p_2)}$	$\frac{K}{s^2+(p_1+p_2)s+(p_1p_2+K)}$
⑧	$\frac{K}{s^2+2\zeta\omega_n s+\omega_n^2}$	$\frac{K}{s^2+2\zeta\omega_n s+(\omega_n^2+K)}$
⑨	$\frac{K(s+z)}{s^2+2\zeta\omega_n s+\omega_n^2}$	$\frac{K(s+z)}{s^2+(2\zeta\omega_n+K)s+(\omega_n^2+Kz)}$
⑩	$\frac{Ks(s+z)}{s^2+2\zeta\omega_n s+\omega_n^2}$	$\frac{K}{K+1}\left[\frac{s(s+z)}{s^2+\frac{2\zeta\omega_n+Kz}{K+1}s+\frac{\omega_n^2}{K+1}}\right]$
⑪	$\frac{K(s^2+2\zeta_N\omega_N s+\omega_N^2)}{s^2+2\zeta_D\omega_D s+\omega_D^2}$	$\frac{K}{K+1}\left[\frac{s^2+2\zeta_N\omega_N s+\omega_N^2}{s^2+\frac{2(\zeta_D\omega_D+\zeta_N\omega_N)}{K+1}s+\frac{(\omega_D^2+\omega_N^2)}{K+1}}\right]$

The magnitude of $G(j\omega)$ is near unity for ω of the order of 10; is much greater than unity for $\omega << 10$; and is much less than unity for $\omega >> 10$. Thus, from 1 and 2 above, three of the four closed-loop denominator factors are approximately $(s + 1)(s + 100)(s + 200)$. Since, for this case, the value of b_{m+n} in Eq. (7) is zero, the negative of the fourth approximate factor is given by $Ka_n/(1)(100)(200) \doteq 10$. The most simply obtained approximate closed-loop factors are than $(s + 1)(s + 10)(s + 100)(s + 200)$.*

Additional approximations, which are especially helpful for those regions of ω where $|G(j\omega)|$ is of the order of unity, can be evolved for many cases by use of the relationships summarized in Table II. The exact relationships between the elementary system open- and closed-loop transfer functions shown there can be interpreted as approximate for more complex systems in regions where the actual system open-loop transfer function is closely similar to an open-loop entry in Table II. Using the same example as above, for the region of ω where $|G(j\omega)|$, is approximately unity, $(\omega \doteq 10)$

$$G(j\omega) \doteq \frac{2 \cdot 10^5\, j\omega}{(j\omega)^2(10^2)(2 \cdot 10^2)} = \frac{10}{j\omega}$$

Using Item (2) in Table II gives $10/(j\omega + 10)$ as an approximation to the closed-loop transfer function for this same ω region. An approximate factor is then $s + 10$. A somewhat closer approximation for both this factor and the one near $|j\omega| = 100$ can be obtained using Item (5) as the open-loop approximation, viz,

$$G(j\omega) \doteq \frac{10^3}{j\omega(j\omega + 100)} \; ; \; G_{rc}(j\omega) \doteq \frac{10^3}{(j\omega)^2 + 100\, j\omega + 1000} = \frac{10^3}{(j\omega + 11.2)(j\omega + 88.7)}$$

Similarly, a better approximation for the root near $j\omega = 1$ can be found by using Item (6) (with $p = 0$), i.e.,

$$G(j\omega) \doteq \frac{2 \cdot 10^5(j\omega + 1)}{(j\omega)^2(100)(200)} = \frac{10(j\omega + 1)}{(j\omega)^2} \; ;$$

$$G_{rc}(j\omega) \doteq \frac{10(j\omega + 1)}{(j\omega)^2 + 10\, j\omega + 10} = \frac{10(j\omega + 1)}{(j\omega + 1.13)(j\omega + 8.87)}$$

In this last expression only the root at $s = -1.13$ is accepted from the approximation since the other open-loop forms used above are more valid for the root near $s = -10$. The differences in the approximate values obtained (i.e., -10, -11.2, -8.87) for this root illustrate the point that judgment is essential in applying this simple, but possibly misleading, technique. When used in conjunction with the graphical techniques discussed in subsequent sections such

---

*An iterative procedure for refining these estimates is presented in References 5 and 6.

guesswork as might be involved in deciding upon the best approximating factors for a given case is alleviated since the appropriate approximation can then be chosen directly from a more complete overall system picture.

The reduction in form of $G(j\omega)$ for local regions of ω can, of course, be carried out using orders higher than the second order forms used above for analytical simplicity. For example, the root near $|j\omega| = 200$ in the illustrative problem can be approximated better by closing the loop around the reduced open-loop transfer function

$$G(j\omega) \doteq \frac{2 \cdot 10^5 \, j\omega}{(j\omega)^2(j\omega + 100)(j\omega + 200)} = \frac{2 \cdot 10^5}{j\omega(j\omega + 100)(j\omega + 200)}$$

The approximate closed-loop transfer function is

$$G_{rc}(j\omega) = \frac{G(j\omega)}{1 + G(j\omega)} \doteq \frac{2 \cdot 10^5}{j\omega(j\omega + 100)(j\omega + 200) + 2 \cdot 10^5}$$

$$\doteq \frac{2 \cdot 10^5}{(j\omega)^3 + 300(j\omega)^2 + 2 \cdot 10^4 \, j\omega + 2 \cdot 10^5}$$

A factor of $(s + 208.9)$ is obtained by factoring the cubic characteristic equation.

An appreciation for the degree of approximation involved in the foregoing is afforded by comparison with the "exact" factors, $(s + 1.125)(s + 10.7)(s + 79.7)(s + 208)$, for this example.

SECTION III

SUMMARY OF ROOT-LOCUS TECHNIQUE

A. GENERAL PRINCIPLES (References 7-10)

The operations of the root-locus method deal directly with the singularities of the open-loop transfer function and generate from these discrete points all loci of closed-loop poles. The equation $1 + G(s) = 0$ is solved by working with the equivalent expression, $G(s) = -1$. Expressing both sides as complex numbers, this can be written

$$|G(s)|\, e^{j\varphi(s)} = e^{j(2k+1)\pi}, \quad k = 0, \pm 1, \pm 2, \cdots \tag{8}$$

requiring simultaneous satisfaction of

$$\varphi(s) = (2k + 1)\pi, \quad k = 0, \pm 1, \pm 2, \cdots \tag{9}$$

and

$$|G(s)| = 1 \tag{10}$$

Each of the components of $G(s)$ given in Eq. (1) can also be interpreted as complex numbers,

$$G(s) = \kappa \frac{\prod_{h=i}^{n} (s + z_h)}{\prod_{i=1}^{m+n} (s + p_i)} = \kappa \left[\frac{\prod_{h=1}^{n} r_{N_h}}{\prod_{i=1}^{m+n} r_{D_i}} \right] e^{j\left(\sum_{h=1}^{n} \varphi_{N_h} - \sum_{i=1}^{m+n} \varphi_{D_i} \right)} \tag{11}$$

where $r_{N_h} = |s + z_h|$, $r_{D_i} = |s + p_i|$, $\varphi_{N_h} = \measuredangle(s + z_h)$, and $\varphi_{D_i} = \measuredangle(s + p_i)$. As vectors on the s-plane typical components of $G(s)$ appear as shown in Fig. 2, with circles and crosses denoting the locations of open-loop zeros and poles, respectively.

In the root-locus method the two conditions, Eq. (9) and (10), are interpreted in a graphical manner using the vector plots described above as a basis. An attempt to determine a root of $1 + G(s)$ is started by choosing a trial value of s (a point on the s-plane) and imagining vectors drawn to this point from each of the poles and zeros of $G(s)$ as illustrated in Fig. 3. Note that all angles are measured in a counterclockwise direction from a horizontal line. When the trial value meets the test

$$\sum_{h=1}^{n} \varphi_{N_h} - \sum_{i=1}^{m+n} \varphi_{D_i} = \begin{cases} (2k + 1)\pi & ; \kappa \text{ positive} \\ \text{or} & \\ 2k\pi & ; \kappa \text{ negative} \end{cases} \tag{12}$$

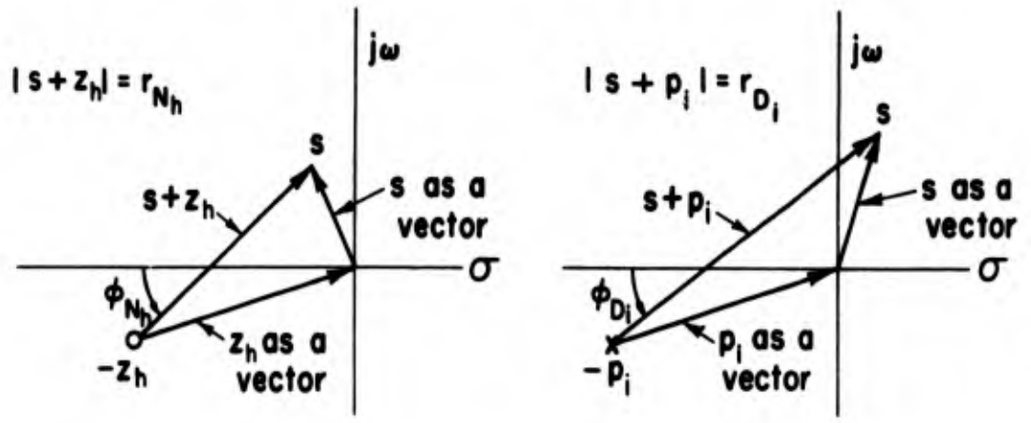

Fig. 2. Vector Plots for Typical Factors of G(s)

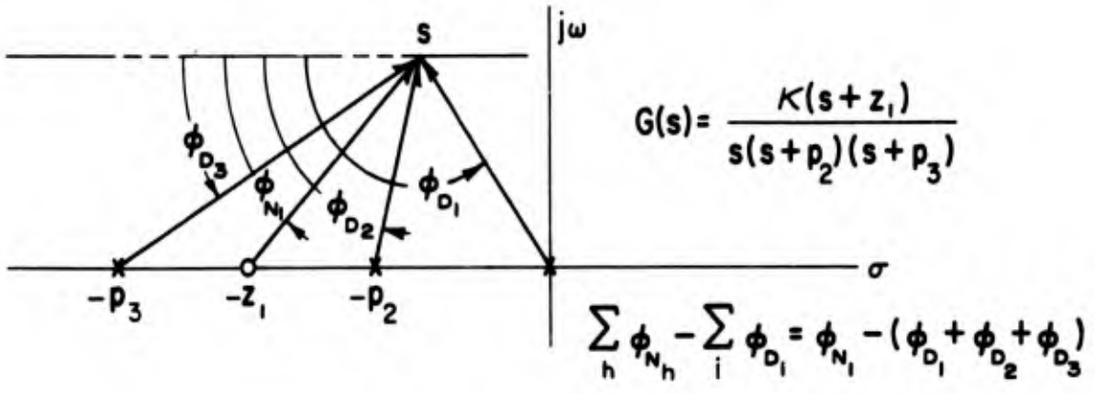

Fig. 3. Angle Measurement Procedure in Root-Locus Construction

then the angle condition, Eq. (9), is satisfied and a possible closed-loop root location has been found. This procedure is repeated a sufficient number of times to establish a series of loci which show all possible closed-loop roots.

The second step of the method is to process the loci determined above into consistent root sets compatible with given values of K. This is accomplished by satisfying the magnitude criterion, Eq. (10), i.e., making

$$|K| \left[\frac{\prod_{h=1}^{n} r_{N_h}}{\prod_{i=1}^{m+n} r_{D_i}} \right] = 1 \tag{13}$$

for the particular values assigned to K. In both steps of the method simple mechanical aids, such as the "Spirule,"* are helpful tools.

A slightly different interpretation of the root-locus criteria statements can be evolved by noting that $G(s) = -1$ is equivalent to

$$\frac{\beta(s)}{\alpha(s)} = -K \tag{14}$$

Since $\beta(s)/\alpha(s)$ is complex, Eq. (14) can be rewritten as

$$\mathrm{Re}\left[\frac{\beta(s)}{\alpha(s)}\right] + j\,\mathrm{Im}\left[\frac{\beta(s)}{\alpha(s)}\right] = -K \tag{15}$$

Since K is real the imaginary term must vanish on the locus of roots. The root-locus criteria statements then become

$$\mathrm{Im}\left[\frac{\beta(s)}{\alpha(s)}\right] = 0 = \mathrm{Im}\left[\beta(s)\alpha^*(s)\right] \tag{16}$$

$$\mathrm{Re}\left[\frac{\beta(s)}{\alpha(s)}\right] = \frac{\mathrm{Re}\left[\beta(s)\alpha^*(s)\right]}{|\alpha(s)|^2} = -K \tag{17}$$

Eq. (16) can be a very useful form when equations for the root locus are desired. These can be obtained simply by substituting $\sigma + j\omega$ for s in Eq. (16), manipulating the result into real and imaginary parts, and setting the latter to zero.

---

*Copyright 1959, North American Aviation, Inc. The Spirule Co., 9728 El Venado, Whittier, Calif.

B. PROPERTIES OF THE LOCUS (References 7-16)

In principle, the above criteria and procedures implicitly contain all the elements of the root-locus method. The construction of a root locus with only this background, however, can require many tedious trial and error attempts. Such painful efforts can be alleviated considerably by a knowledge of general and special loci properties. For systems where the form of G(s) is given by Eq. (1), general loci characteristics are such that:

1. The total number of separate loci branches, each representing a zero of $1 + G(s)$, is equal to the total number of open-loop poles (m+n).

2. The root loci are symmetrical about the real ($\omega = 0$) axis.

3. The starting points (i.e., those points which represent roots of $\beta(s) + \kappa\alpha(s)$ when κ approaches zero) of the loci branches are the open-loop poles.

4. The end or termination points (i.e., roots of $\beta(s) + \kappa\alpha(s)$ as κ approaches infinity) for the branches are the open-loop zeros and points at infinity.

   a. n (the total number of zeros) branches of the loci terminate at open-loop zeros.

   b. m branches proceed to infinity approaching linear asymptotes which are centered at a point on the real axis given by

$$\sigma_A = -\frac{\sum_{i=1}^{m+n} p_i - \sum_{j=1}^{n} z_j}{m} = -\frac{b_1 - a_1}{m} \tag{18}$$

   and make angles with the real axis of

$$\varphi_A = \begin{cases} \dfrac{(2k+1)\pi}{m} & ; \kappa \text{ positive} \\ \text{or} & k = 0, \pm 1, \pm 2, \cdots \\ \dfrac{2k\pi}{m} & ; \kappa \text{ negative} \end{cases} \tag{19}$$

5. At junction points the tangents to the loci are equally spaced over 2π radians.

6. The angle of locus departure (from a pole) or arrival (at a zero) is the difference between the criterion angle [$(2k+1)\pi$ and $2k\pi$ for κ positive and negative, respectively] and the net angle (measured at the pole or zero under consideration) due to all the other poles

and zeros. The consequences of this property are illustrated in Fig. 4 for several simple pole-zero configurations.

7. The root locus on the real axis lies along alternate segments connecting the real poles and zeros. When K is positive (negative) loci exist in all intervals along the axis where there is an odd (even) total number of poles and zeros to the right of the interval.

8. Locus breakaway from the real axis occurs where the net change in angle caused by a small vertical displacement is zero. These points also correspond to real roots of:

   a. $\frac{dG(s)}{ds} = 0$ or its equivalent

   $$\alpha(s)\frac{d\beta(s)}{ds} = \beta(s)\frac{d\alpha(s)}{ds} \tag{20}$$

   b. $$\mathrm{Im}\left[\frac{\beta(s)}{\alpha(s)}\right]_{\omega=0} = \mathrm{Im}\left[\beta(s)\alpha^*(s)\right]_{\omega=0} = 0 \tag{21}$$

9. Locus crossings of the imaginary axis occur when $\mathrm{Im}\left[\beta(s)/\alpha(s)\right]_{\sigma=0}$ is zero. Such points correspond to neutral stability points as determined by the Routh or similar stability criterion.

10. When a complete set of closed-loop roots is available for some value of K, these roots may be used in the same fashion as open-loop roots for purposes of continuing the plot.

To illustrate some of these properties consider the open-loop transfer function

$$G(s) = \frac{K}{s(s+a)(s+b)}$$

To find the locus, Eq. (16) is applied.

$$\mathrm{Im}\left[\frac{\beta(s)}{\alpha(s)}\right] = \mathrm{Im}\left[(j\omega+\sigma)(j\omega+\sigma+a)(j\omega+\sigma+b)\right]$$

$$= \omega\left\{-\omega^2 + \left[3\sigma^2 + 2(a+b)\sigma + ab\right]\right\}$$

$$= 0$$

So the locus is given by

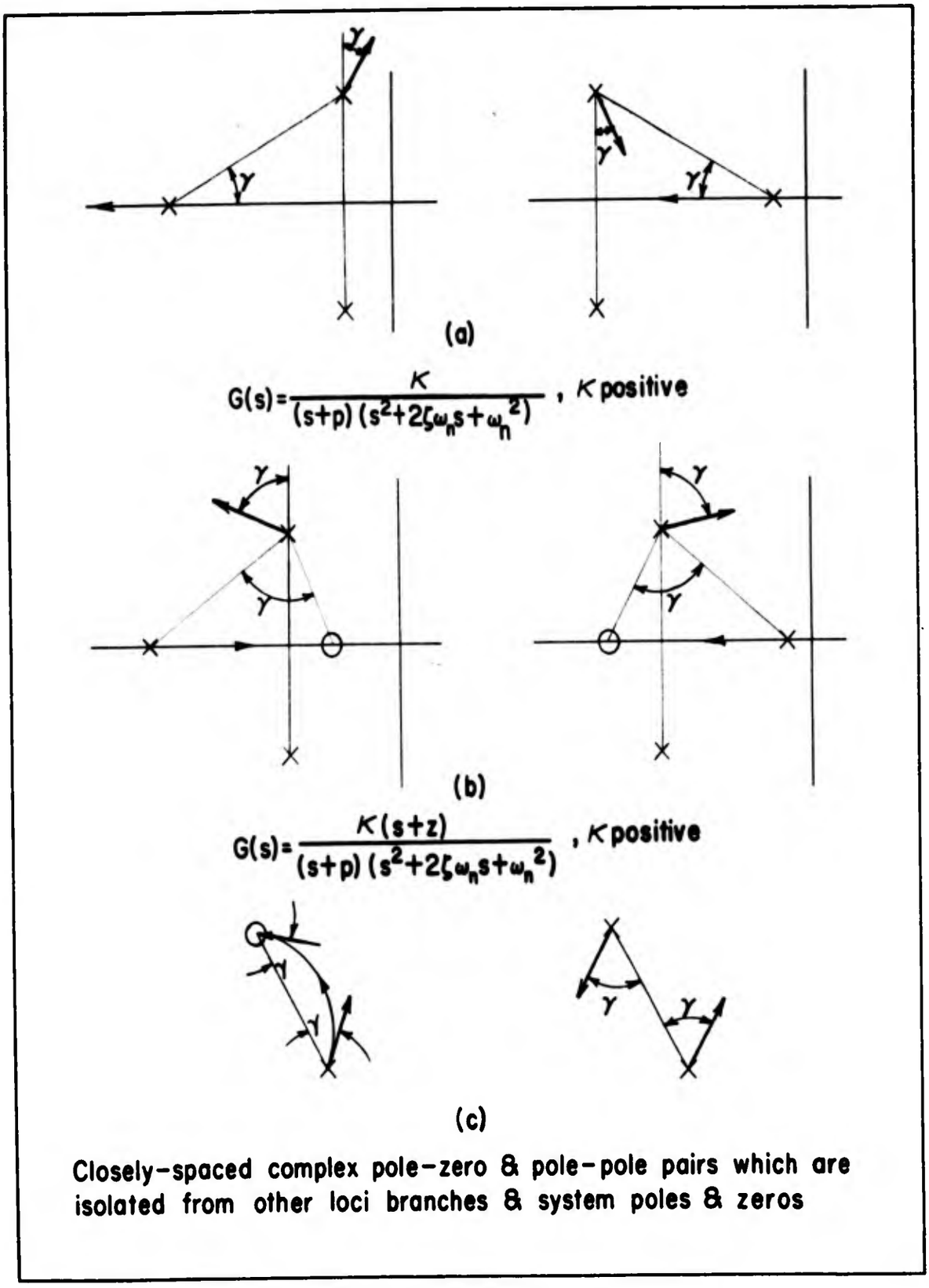

Fig. 4. Illustrative Root-Locus Departure Angles

$$\omega = 0$$

$$\omega^2 = 3\sigma^2 + 2(a + b)\sigma + ab$$

The latter equation, after a few manipulations, can be put into the conventional form for a hyperbola,

$$\left[\frac{\sigma + \frac{1}{3}(a + b)}{\frac{1}{3}\sqrt{a^2 - ab + b^2}}\right]^2 - \left[\frac{\omega}{\frac{\sqrt{3}}{3}\sqrt{a^2 - ab + b^2}}\right]^2 = 1$$

For higher order systems the locus equations are not too helpful in the construction process, which is ordinarily performed with the "Spirule" or other aids.

The real axis breakaway can be easily computed using Eq. (21), and the above expression for $\mathrm{Im}[\beta(s)/\alpha(s)]$, i.e.,

$$\sigma_b^2 + \frac{2}{3}(a + b)\sigma_b + \frac{ab}{3} = 0$$

$$\sigma_b = -\frac{1}{3}\left[(a + b) \pm \sqrt{a^2 - ab + b^2}\right]$$

The plus sign for the radical is used when K is negative, and the minus sign when K is positive.

The intersection of the asymptotes on the real axis occurs at, from Eq. (18),

$$\sigma_A = -\frac{(a + b)}{3}$$

and the angles of the asymptotes, for K positive, are, from Eq. (19),

$$\varphi_A = \frac{(2k + 1)\pi}{3} = \pm\frac{\pi}{3}, \pi$$

The locus will cross the imaginary axis when $\mathrm{Im}\left[\beta(s)/\alpha(s)\right]_{\sigma=0}$ is zero, or when

$$\omega^2 = ab$$

The gain at this neutral stability point, as determined by the Routh criterion (Reference 1), will be

$$K = ab(a + b)$$

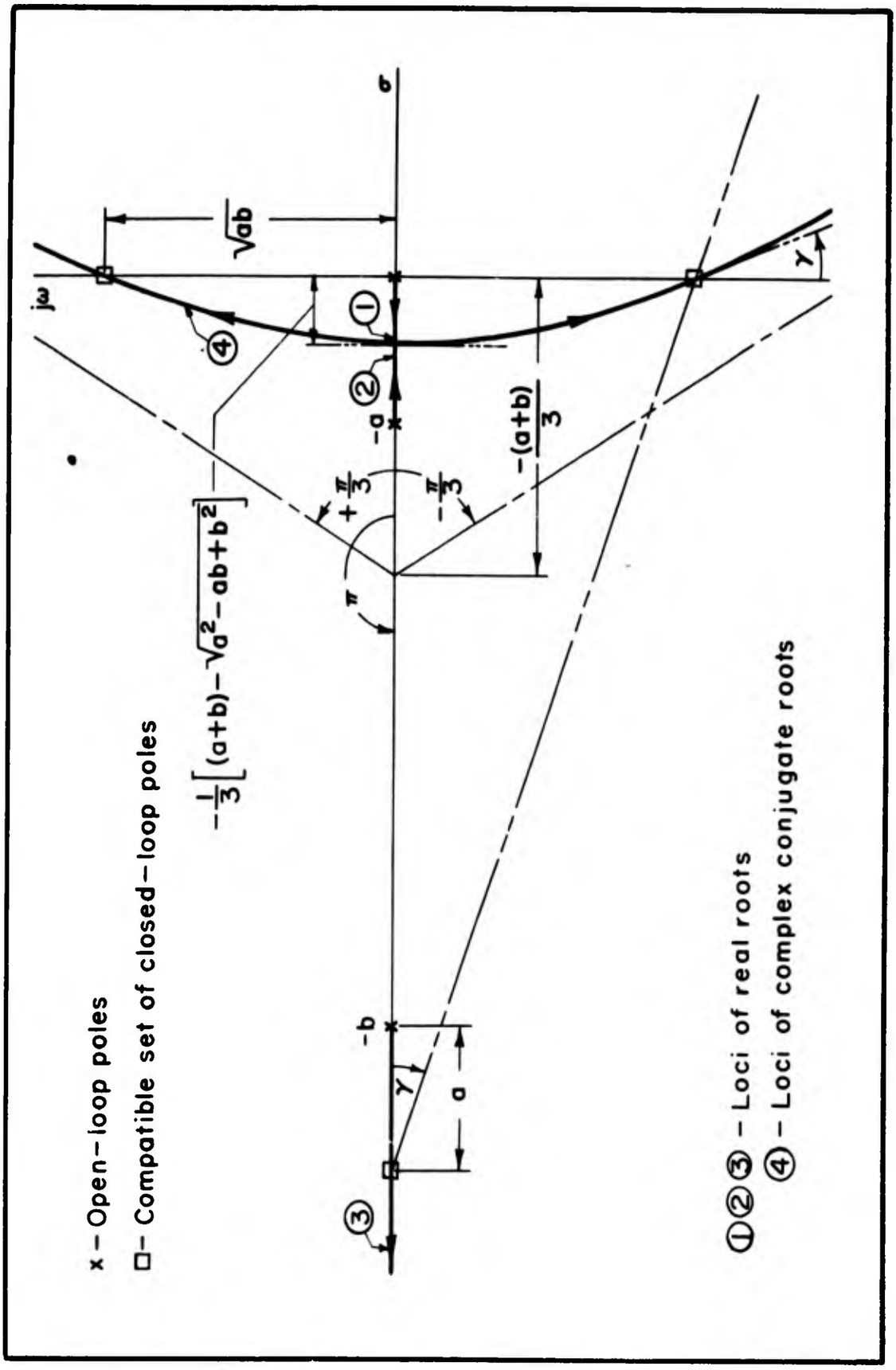

Fig. 5. Illustrative Root Locus for $G(s) = \frac{K}{s(s+a)(s+b)}$

The complete root locus is shown in Fig. 5. The simple properties computed above are illustrated, property 10 is used in determining the angle γ, and Eq. (5) is used in determining the third root at crossover gain.

Because a knowledge of elementary cases is helpful in bolstering intuitive processes, three additional simple cases are shown in Fig. 6.

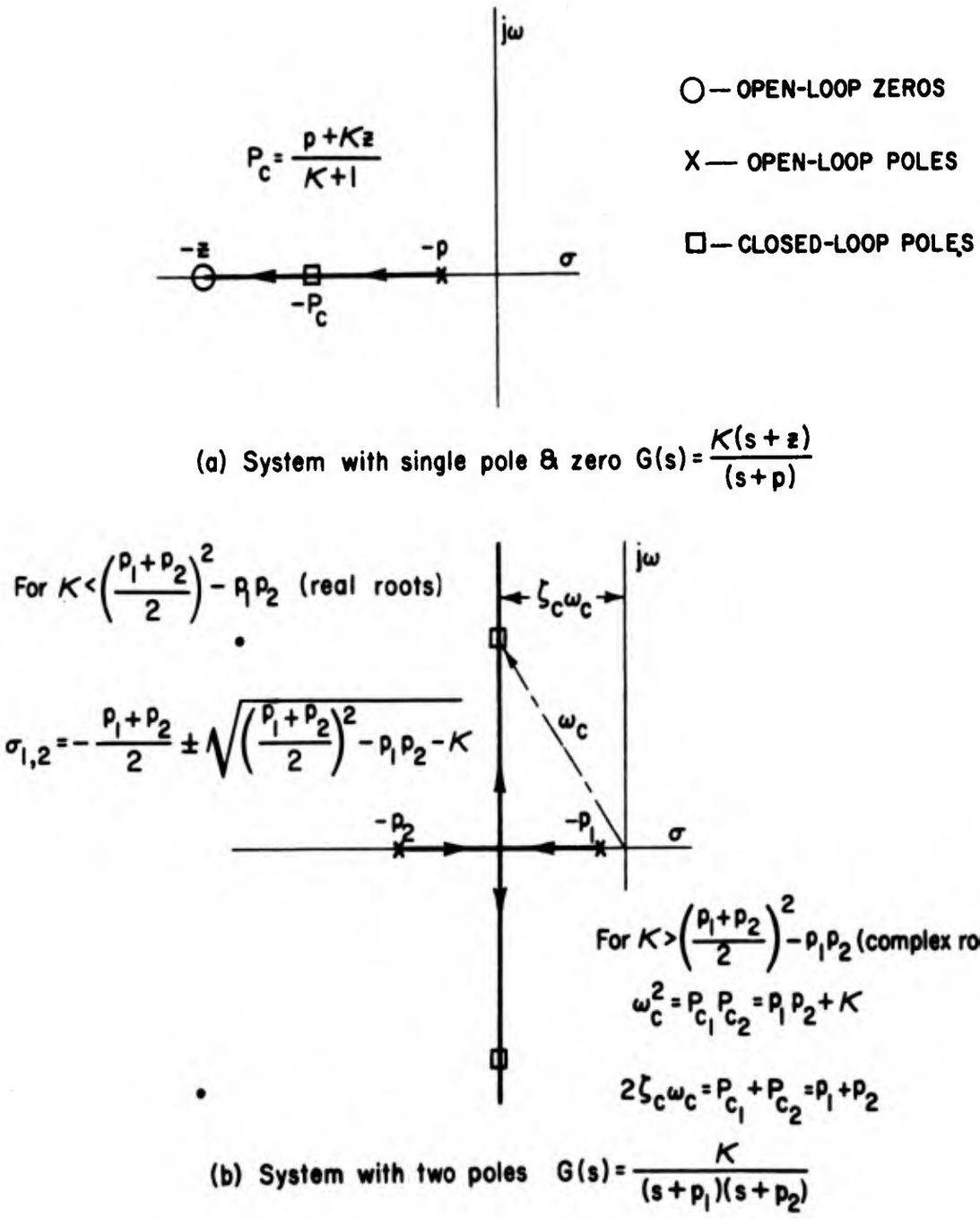

Fig. 6. Root Loci for Simple Systems

For $K<4(z-p)$,(complex roots)

$2\zeta_c\omega_c = P_{c_1} + P_{c_2} = 2p+K$

$\omega_c^2 = P_{c_1}P_{c_2} = p^2+Kz$

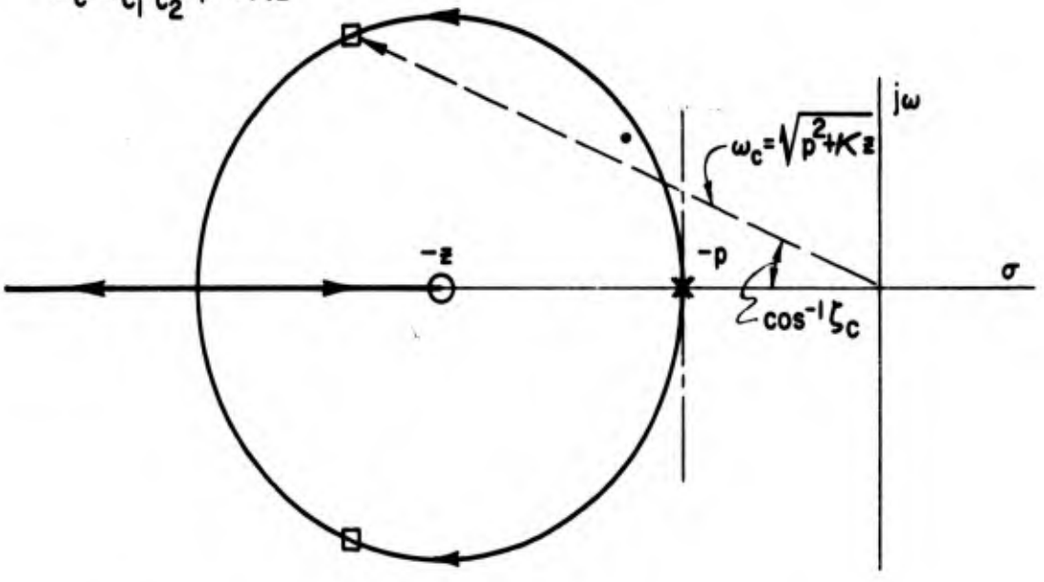

For $K>4(z-p)$,(real roots)

$$\sigma_{1,2} = -\frac{(2p+K)}{2} \pm \sqrt{\left(\frac{2p+K}{2}\right)^2 - (p^2+Kz)}$$

(c) System with lead & second order pole $G(s) = \dfrac{K(s+z)}{(s+p)^2}$; $z > p$

Fig. 6 (Concluded). Root Loci for Simple Systems

SECTION IV

THE LOGARITHMIC G(s) METHODS

A. GENERAL

In the logarithmic G(s) methods closed-loop poles are found by operations upon graphical forms of the open-loop transfer function G(s) considered as a continuous function of s. Starting with such representations of G(s), either of two procedures can be carried out. For the first, the G(s) form only is required, and closed-loop poles are found simply by noting when the conditions $G(s) = -1$ are fulfilled. The second procedure, which can be far more rapid, involves two steps: (1) development of a closed-loop transfer function form and (2) decomposition of this closed-loop form into its constituent poles and zeros. In principle this latter process could be performed with any one of a variety of G(s) graphical representations, all of which implicitly contain the total information about the singularities and gain. In practice, of course, efficiency will depend greatly upon the form of plot initially adopted to denote G(s). First consideration must be given, therefore, to the selection of graphical configurations which are best suited as practical means for the kinds of operations required by the procedures mentioned above.

Since many forms of transfer function plot are possible, yet not all equally useful in a practical context, it is pertinent to specify those features which are either mandatory in order to perform the required operations, or desirable for ease of manipulation and interpretation. Among these are:

Clarity - - - - - - The plot should show clearly the characteristics (gain, poles, and zeros) of the transfer function.

Operability - - - - Construction of a particular transfer function, and the manipulative processes involved in combining, by addition or multiplication, two or more transfer functions, should be simple operations.

Decomposability - - The inverse process in going from the plot to the analytical form of the transfer function should be straightforward.

Interpretability - The plot should have a simple physical interpretation in terms of possible tests performed on actual equipment.

Unfortunately no single form of G(s) plot possesses all of these properties to a degree which is completely satisfactory. However, Bode diagrams (Reference 17) comprising plots of amplitude ratio [expressed as $20 \log |G(s)|$] and phase, $\angle G(s)$, versus the log of selected values of s, come close to the ideal.

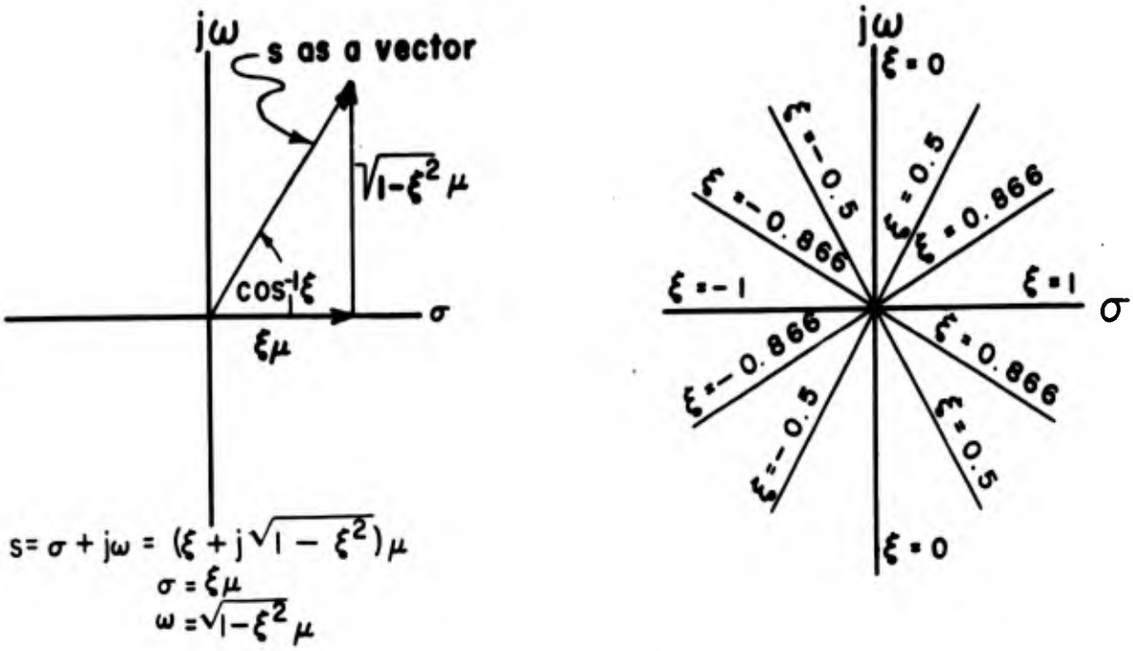

(a) Linear connection between ω and σ, and s-plane loci with $\frac{\sigma}{\omega}$ = constant

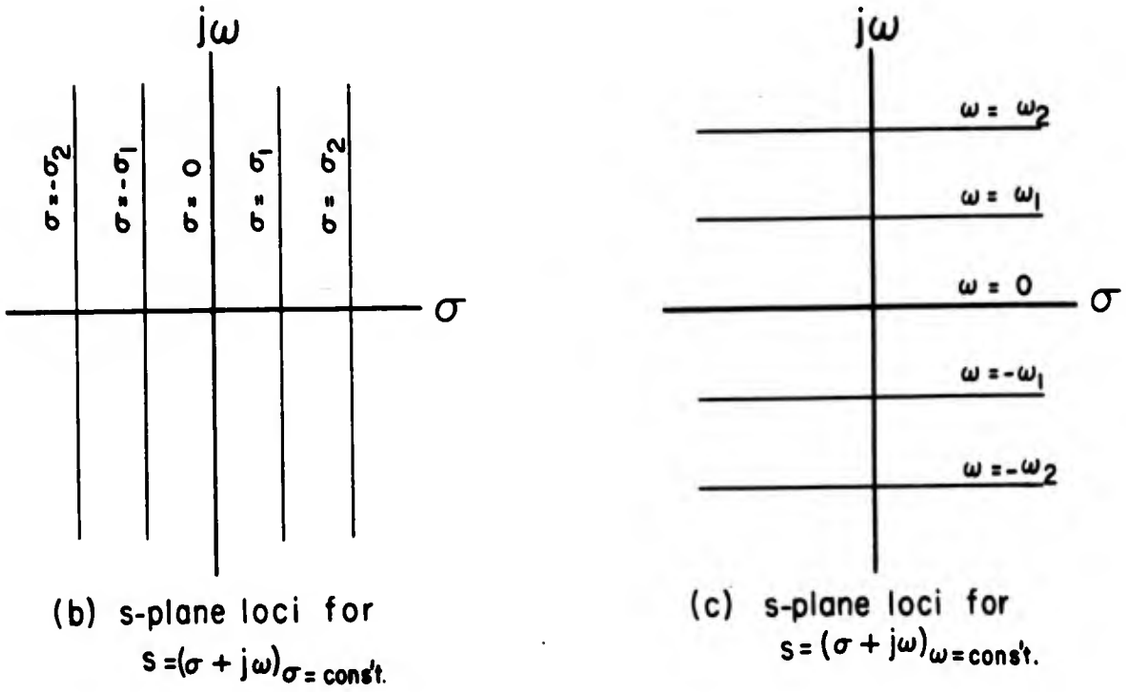

(b) s-plane loci for $s=(\sigma+j\omega)_{\sigma=\text{const.}}$

(c) s-plane loci for $s=(\sigma+j\omega)_{\omega=\text{const.}}$

Fig. 7. s-Plane Loci for Various Special Values of s

For a given value of s, G(s) is a complex number which can be expressed as a magnitude (amplitude ratio) and phase angle. The variable s is itself complex ($\sigma + j\omega$), so a plot of G(s) as a continuous function of s would, in general, require four dimensions or two plots each of three dimensions (e.g., $|G(s)|$ vs s and $\measuredangle G(s)$ vs s). The graphical requirements can be reduced to one plot of three or two plots of two dimensions by connecting σ and ω linearly, i.e., letting

$$s = \left(\xi + j\sqrt{1 - \xi^2}\right)\mu, \xi = \text{constant};\ \sigma = \xi\mu,\ \omega = \sqrt{1 - \xi^2}\,\mu;\ |s| = \mu;$$

or by holding either σ or ω constant while the other is allowed to vary. Fig. 7 shows these possibilities in the s-plane. The simplest form of s is $s = \pm\sigma$ and $s = \pm j\omega$, which correspond to $\xi = \pm 1$ and $\xi = 0$, respectively.

All of the G(s) functions based upon specializing the values assigned to s possess useful physical interpretations. $G(\pm j\omega)$, $G(\pm\sigma)$, $G\left(\xi\mu + j\mu\sqrt{1 - \xi^2}\right)$, for example, are related to the particular integral component of the open-loop system time response obtained when the open-loop system is excited by a sinusoidal, exponential, or damped sinusoidal input, respectively. The simplest open-loop transfer function forms are obtained, of course, when $s = \pm\sigma$ and $s = \pm j\omega$. When $G(\pm j\omega)$ is used, considerable theoretical advantage can accrue since it allows essentially all of "frequency domain" theory (e.g., Reference 17) to be applied to other aspects of linear feedback systems problems. For the present parochial view of the analysis problem, however, this latter point is of little interest and can even be a detriment if it tends to de-emphasize the view of $G(\pm j\omega)$ as simply a specialized form of the more general transfer function G(s).

B. PROPERTIES OF CONTINUOUS G(s) BODE PLOTS

The form of the open-loop transfer function, Eq. (1), can be modified to:

$$G(s) = \frac{KA(s)}{s^k B(s)}$$

$$= \frac{K \prod_{j=1}^{w}\left[\left(\frac{s}{\omega_j}\right)^2 + \frac{2\zeta_j s}{\omega_j} + 1\right] \prod_{j=2w}^{n} (T_j s + 1)}{s^k \prod_{i=1}^{v}\left[\left(\frac{s}{\omega_i}\right)^2 + \frac{2\zeta_i s}{\omega_i} + 1\right] \prod_{i=2v}^{m+n-k} (T_i s + 1)} \qquad (22)$$

where the ζ's, ω's, T's, and K are real constants, and k is not necessarily positive. The natural logarithm of Eq. (22) is

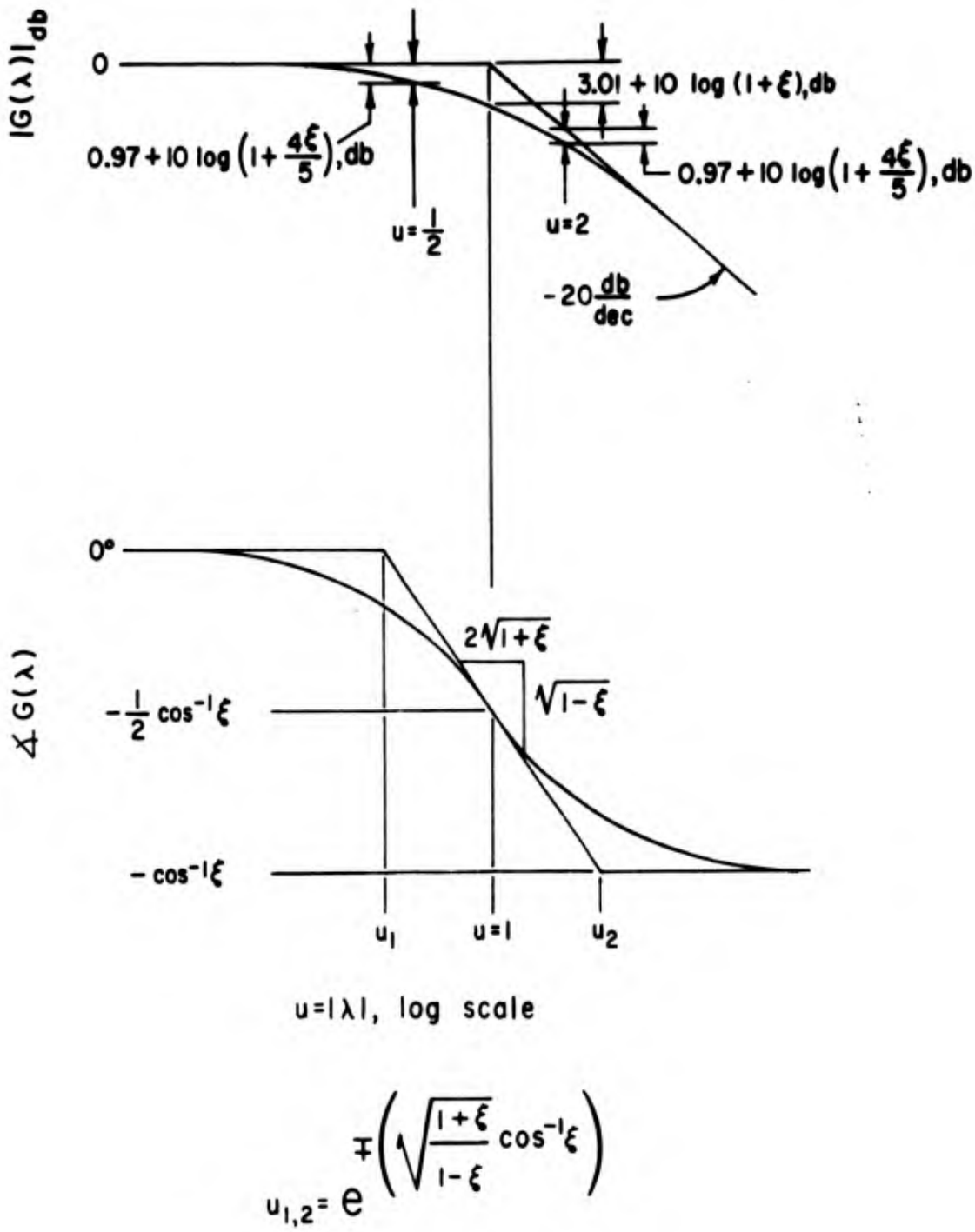

Fig. 8. Elementary Properties of the First Order Pole $G(\lambda) = \frac{1}{\lambda + 1}$

$$\ln G(s) = \left\{ \ln K + \sum_{j=1}^{w} \ln \left| \left(\frac{s}{\omega_j}\right)^2 + \frac{2\zeta_j s}{\omega_j} + 1 \right| + \sum_{j=2w}^{n} \ln \left| T_j s + 1 \right| \right.$$

$$\left. - k \ln |s| - \sum_{i=1}^{v} \ln \left| \left(\frac{s}{\omega_i}\right)^2 + \frac{2\zeta_i s}{\omega_i} + 1 \right| - \sum_{i=2v}^{m+n-k} \ln \left| T_i s + 1 \right| \right\}$$

$$+ \sqrt{-1} \left\{ \sum_{j=1}^{w} \tan^{-1} \frac{\mathrm{Im}\left[\left(\frac{s}{\omega_j}\right)^2 + \frac{2\zeta_j s}{\omega_j}\right]}{1 + \mathrm{Re}\left[\left(\frac{s}{\omega_j}\right)^2 + \frac{2\zeta_j s}{\omega_j}\right]} + \sum_{j=2w}^{n} \tan^{-1} \frac{\mathrm{Im}\, T_j s}{1 + \mathrm{Re}\, T_j s} \right.$$

$$- k \tan^{-1} \frac{\mathrm{Im}\, s}{\mathrm{Re}\, s} - \sum_{i=1}^{v} \tan^{-1} \frac{\mathrm{Im}\left[\left(\frac{s}{\omega_i}\right)^2 + \frac{2\zeta_i s}{\omega_i}\right]}{1 + \mathrm{Re}\left[\left(\frac{s}{\omega_i}\right)^2 + \frac{2\zeta_i s}{\omega_i}\right]}$$

$$\left. - \sum_{i=2v}^{m+n-k} \tan^{-1} \frac{\mathrm{Im}\, T_i s}{1 + \mathrm{Re}\, T_i s} \right\}$$

$$= \ln |G(s)| + j \measuredangle G(s) \qquad (23)$$

In the conventional Bode diagram representation of G(s) the logarithmic magnitude, $\ln |G(s)|$, is first modified to decibels by replacing the natural logarithm with 20 $\log_{10}$, and the result is plotted versus $\log |s|$. The "phase," $\measuredangle G(s)$ in degrees, is plotted separately against $\log |s|$. To simplify the notation 20 $\log_{10}$, $|G(s)|$ will be abbreviated as $|G(s)|_{db}$, and will be called the db amplitude ratio.

The most striking features of the first and second order constituents of Eq. (23) in such plots are their asymptotic and symmetric characteristics. Normalized first and second order factors can be obtained from $[Ts + 1]^{\pm 1}$ and $\left[\frac{s^2}{\omega_n^2} + \frac{2\zeta s}{\omega_n} + 1\right]^{\pm 1}$ by letting $s = \frac{\lambda}{T}$ and $s = \omega_n \lambda$, respectively. The normalized factors then become $[\lambda + 1]^{\pm 1}$ and $[\lambda^2 + 2\zeta\lambda + 1]^{\pm 1}$. Log $|s|$, when normalized in the same fashion, becomes $\log |\lambda| = \log u$, where $\lambda = \left(\xi + j\sqrt{1 - \xi^2}\right)u$ in general. When plotted against log u, the db amplitude ratios and phases of the normalized first and second order factors possess the following distinctive characteristics (refer to Figs. 8 and 9)

db Amplitude Ratio

1. Straight line asymptotes are zero db and have slopes of zero db/decade when $u \ll 1$ for both forms. Slopes are ±20 db/decade for first order and ±40 db/decade for second order when $u \gg 1$. Intersection of the asymptotes occurs

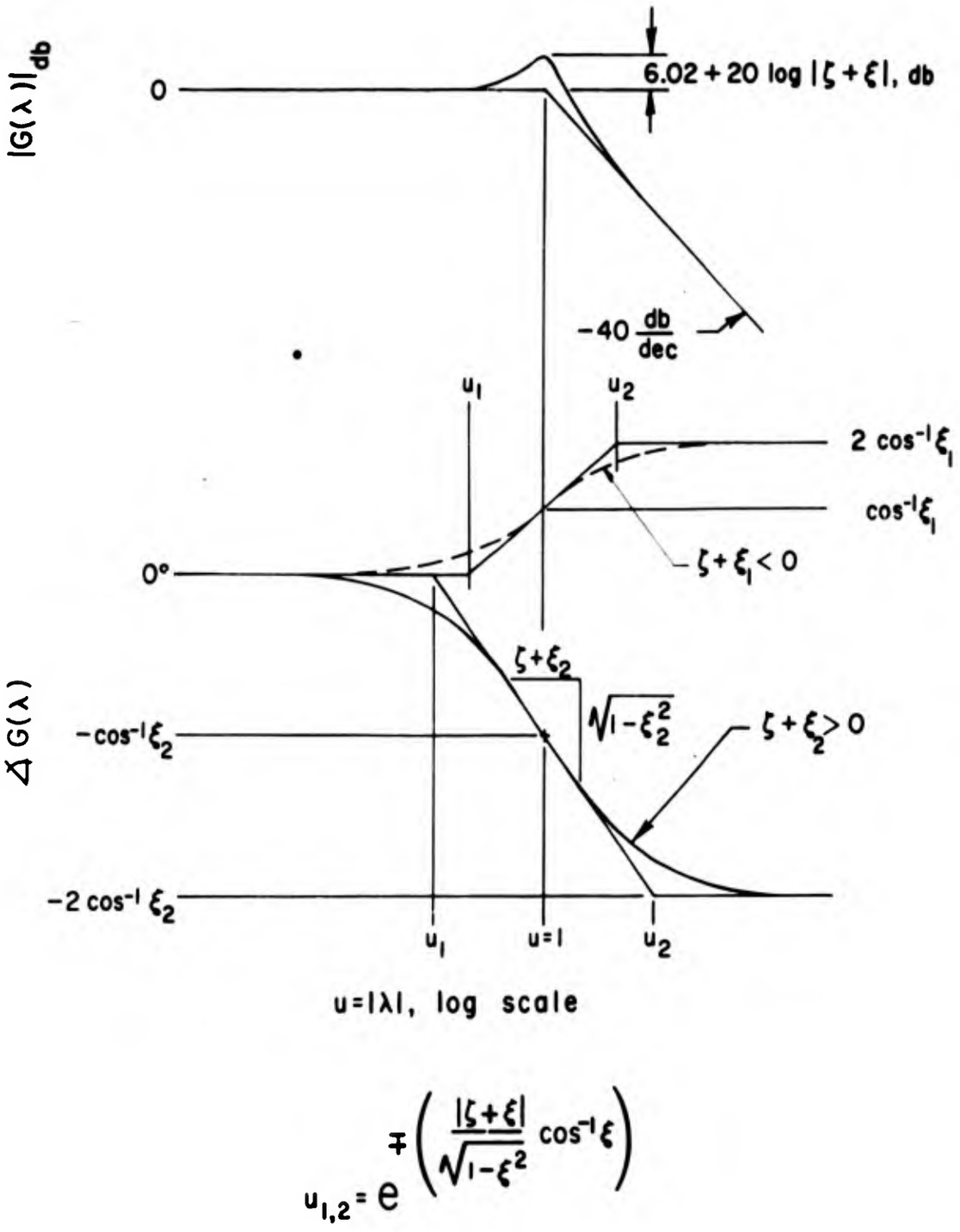

Fig. 9. Elementary Properties of the Second Order Pole $G(\lambda) = \dfrac{1}{\lambda^2 + 2\zeta\lambda + 1}$

at u = 1. The relative direction of the slope change is negative for a pole and positive for a zero.

2. Departure of the actual db amplitude ratio from the asymptotes is symmetrical (even) with log u about u = 1.

Phase

1. Straight line asymptotes have slopes of zero degrees/decade when $u \ll 1$ and $u \gg 1$ for both forms. An intermediate asymptote, tangent to the actual phase at u = 1, has the slope $\pm(1/2)\sqrt{1 - \xi}/\sqrt{1 + \xi}$ for first orders and $\pm\sqrt{1 - \xi^2}/(\zeta + \xi)$ for second orders. The phase for $u \ll 1$ approaches zero degrees, while that for $u \gg 1$ approaches $\pm\cos^{-1}\xi$ for the first order and $\pm 2\cos^{-1}\xi$ for the second order terms.

2. Departures of the actual phase from the asymptotes are odd with log u about u = 1.

Other properties of importance for first order terms are illustrated by Fig. 8 or tabulated in Table III. Similar features for second order factors appear in Fig. 9 and Table IV.

It is especially noteworthy that quantities which define poles and zeros are reflected explicitly at certain key points on G(s) plots. For instance, the magnitude of the inverse time constant (for first order) or undamped natural frequency (for second order) determines the location of the db amplitude ratio break point (intersection of the db amplitude ratio asymptotes). For second order terms the magnitude of the damping ratio uniquely determines the departure of $|G(j\omega)|_{db}$ and $|G(-\sigma)|_{db}$ from the break point, as well as the maximum db amplitude ratio departures. The values of these departures are:

Departure from the Break Point

$$|G(j\omega)|_{db} = \pm\left(|2\zeta|_{db}\right) \quad , \text{at } \omega = \omega_n$$

$$|G(-\sigma)|_{db} = \pm\left(|2(1-\zeta)|_{db}\right), \text{ at } \sigma = \omega_n$$

Maximum Departure from the Asymptotes

$$|G(j\omega)|_{db} = \pm\left(|2\zeta\sqrt{1 - \zeta^2}|_{db}\right), \text{ at } \omega = \omega_n\sqrt{1 - 2\zeta^2} = \omega_p$$

$$|G(-\sigma)|_{db} = \pm\left(|1 - \zeta^2|_{db}\right) \quad , \text{at } \sigma = \omega_n\zeta$$

where the plus sign applies with a zero, and the minus sign with a pole. Further, both magnitude and sign of the damping ratio enter into the phase slope of $\angle G(j\omega)$ at the break point of the amplitude ratio's asymptote.

Unlike the asymptotic db amplitude ratio plots, which have only one break point and are independent of ξ, the phase asymptotes in general break twice and

TABLE III-A

AMPLITUDE RATIO PROPERTIES FOR $G(\lambda) = \lambda + 1$

$$\lambda = \left(\xi + j\sqrt{1 - \xi^2}\right)u$$

	$\left\|G(\lambda)\right\| = \sqrt{1 + 2\xi u + u^2}$		
	General	$\xi = 0$ $\left\|G(\lambda)\right\| = \sqrt{1 + u^2}$	$\xi = \pm 1$ $\left\|G(\lambda)\right\| = 1 \pm u$
$u \ll 1$	$1 + \xi u$	1	$1 \pm u$
$u = 1$	$\sqrt{2(1 + \xi)}$	$\sqrt{2}$	1 ± 1
$u \gg 1$	$u + \xi$	u	$u \pm 1$

	$\frac{d \ln\left\|G(\lambda)\right\|}{d \ln u} = \frac{u(\xi + u)}{1 + 2\xi u + u^2}$		
	General	$\xi = 0$ $\frac{d \ln\left\|G(\lambda)\right\|}{d \ln u} = \frac{u^2}{1 + u^2}$	$\xi = \pm 1$ $\frac{d \ln\left\|G(\lambda)\right\|}{d \ln u} = \frac{u}{u \pm 1}$
$u \ll 1$	$u\left[\xi + (1 - 2\xi^2)u\right]$	u^2	$u(\pm 1 - u)$
$u = 1$	$\frac{1}{2}$	$\frac{1}{2}$	$\frac{1}{1 \pm 1}$
$u \gg 1$	$1 - \frac{\xi}{u}$	1	$1 \mp \frac{1}{u}$

TABLE III-B

PHASE PROPERTIES FOR $G(\lambda) = \lambda + 1$

$$\lambda = \left(\xi + j\sqrt{1 - \xi^2}\right)u$$

	$\measuredangle G(\lambda) = \tan^{-1} \frac{u\sqrt{1 - \xi^2}}{1 + \xi u}$		
	General	$\xi = 0$ $\measuredangle G(\lambda) = \tan^{-1} u$	$\xi = \pm 1$ $\measuredangle G(\lambda) = \tan^{-1} \frac{0}{1 \pm u}$
$u \ll 1$	$u\sqrt{1 - \xi^2}(1 - \xi u)$	u	0
$u = 1$	$\frac{1}{2}\cos^{-1}\xi$	$\frac{\pi}{4}$	$\frac{\pi}{4} \mp \frac{\pi}{4}$
$u \gg 1$	$\tan^{-1}\frac{\sqrt{1 - \xi^2}}{\xi + \frac{1}{u}}$	$\frac{\pi}{2} - \frac{1}{u}$	$\frac{\pi}{2} \mp \frac{\pi}{2}$

	$\frac{d \measuredangle G(\lambda)}{d \ln u} = \frac{u\sqrt{1 - \xi^2}}{1 + 2\xi u + u^2}$		
	General	$\xi = 0$ $\frac{d \measuredangle G(\lambda)}{d \ln u} = \frac{u}{1 + u^2}$	$\xi = \pm 1$ $\frac{d \measuredangle G(\lambda)}{d \ln u} = \frac{0}{(1 \pm u)^2}$
$u \ll 1$	$u\sqrt{1 - \xi^2}(1 - 2\xi u)$	u	0
$u = 1$	$\frac{1}{2}\sqrt{\frac{1 - \xi}{1 + \xi}}$	$\frac{1}{2}$	$0 (\xi = +1)$ $\infty (\xi = -1)$
$u \gg 1$	$\frac{\sqrt{1 - \xi^2}}{u + 2\xi}$	$\frac{1}{u}$	0

TABLE IV-A

AMPLITUDE RATIO PROPERTIES FOR $G(\lambda) = \lambda^2 + 2\xi\lambda + 1$

$$\lambda = (\xi + j\sqrt{1-\xi^2})u$$

$$|G(\lambda)| = \left\{[1 + 2(\zeta\xi + \sqrt{(1-\zeta^2)(1-\xi^2)})u + u^2][1 + 2(\zeta\xi - \sqrt{(1-\zeta^2)(1-\xi^2)})u + u^2]\right\}^{1/2}$$

	General	$\xi = 0$ $\lvert G(\lambda)\rvert = [1 + 2(2\zeta^2-1)u^2 + u^4]^{1/2}$	$\xi = \pm 1$ $\lvert G(\lambda)\rvert = 1 \pm 2\zeta u + u^2$
$u \ll 1$	$1 + 2\zeta\xi u$	1	$1 \pm 2\zeta u$
$u = 1$	$\lvert 2(\zeta + \xi)\rvert$	$\lvert 2\zeta\rvert$	$2(1 \pm \zeta)$
$u \gg 1$	$u^2(1 + \frac{2\zeta\xi}{u})$	u^2	$u^2(1 \pm \frac{2\zeta}{u})$

$$\frac{d \ln |G(\lambda)|}{d \ln u} = u\left\{\frac{\zeta\xi + \sqrt{(1-\zeta^2)(1-\xi^2)} + u}{1 + 2(\zeta\xi + \sqrt{(1-\zeta^2)(1-\xi^2)})u + u^2} + \frac{\zeta\xi - \sqrt{(1-\zeta^2)(1-\xi^2)} + u}{1 + 2(\zeta\xi - \sqrt{(1-\zeta^2)(1-\xi^2)})u + u^2}\right\}$$

	General	$\xi = 0$ $\frac{d \ln \lvert G(\lambda)\rvert}{d \ln u} = \frac{2u^2[(2\zeta^2-1)+u^2]}{1+2(2\zeta^2-1)u^2+u^4}$	$\xi = \pm 1$ $\frac{d \ln \lvert G(\lambda)\rvert}{d \ln u} = \frac{2u(u\pm\zeta)}{1\pm 2\zeta u+u^2}$
$u \ll 1$	$2u\{\zeta\xi + [2\zeta^2 + 2\xi^2 - 4\zeta^2\xi^2 - 1]u\}$	$2(2\zeta^2 - 1)u^2$	$2u[\pm\zeta + (1 - 2\zeta^2)u]$
$u = 1$	1	1	1
$u \gg 1$	$2(1 - \frac{\zeta\xi}{u})$	2	$2(1 \mp \frac{\zeta}{u})$

TABLE IV-B

PHASE PROPERTIES FOR $G(\lambda) = \lambda^2 + 2\zeta\lambda + 1$

$\lambda = (\xi + j\sqrt{1 - \xi^2})u$

$$|\angle G(\lambda)|^* = \tan^{-1} \frac{2u\sqrt{1 - \xi^2}\,(\xi u + \zeta)}{1 + 2\zeta\xi u + (2\xi^2 - 1)u^2}$$

	General	$\xi = 0$ $\angle G(\lambda) = \tan^{-1} \frac{2u\zeta}{1-u^2}$	$\xi = \pm 1$ $\angle G(\lambda) = \frac{0}{1 \pm 2\zeta u + u^2}$
$u \ll 1$	$2u\sqrt{1-\xi^2}\,[\zeta + \xi(1-2\zeta^2)u]$	$2\zeta u$	0
$u = 1$	$\cos^{-1}\xi$	$\frac{\pi}{2}$	$0\ (\zeta \neq \mp 1)$
$u \gg 1$	$\tan^{-1} \frac{\sqrt{1 - \xi^2}}{\xi\left[1 - \frac{1}{2\xi(\xi + \frac{\zeta}{u})}\right]}$	$\pi - \frac{2\zeta}{u}$	0

$$\left|\frac{d\angle G(\lambda)}{d \ln u}\right|^* = \frac{2u\sqrt{1 - \xi^2}\,(\zeta + 2\xi u + \zeta u^2)}{|G(\lambda)|^2}$$

	General	$\xi = 0$ $\frac{2u\zeta(1 + u^2)}{[1 + 2(2\zeta^2 - 1)u^2 + u^4]}$	$\xi = \pm 1$ $\frac{0}{1 \pm 2\zeta u + u^2}$
$u \ll 1$	$2u\sqrt{1-\xi^2}\,[\zeta + 2\xi(1-2\zeta^2)u]$	$2\zeta u$	0
$u = 1$	$\frac{\sqrt{1 - \xi^2}}{(\zeta + \xi)}$	$\frac{1}{\zeta}$	$0\ (\zeta \neq \mp 1)$
$u \gg 1$	$\frac{2\sqrt{1-\xi^2}}{u^2}\,[\zeta u + 2\xi(1-2\zeta^2)]$	$\frac{2\zeta}{u}$	0

*See Fig. 9 for sign convention.

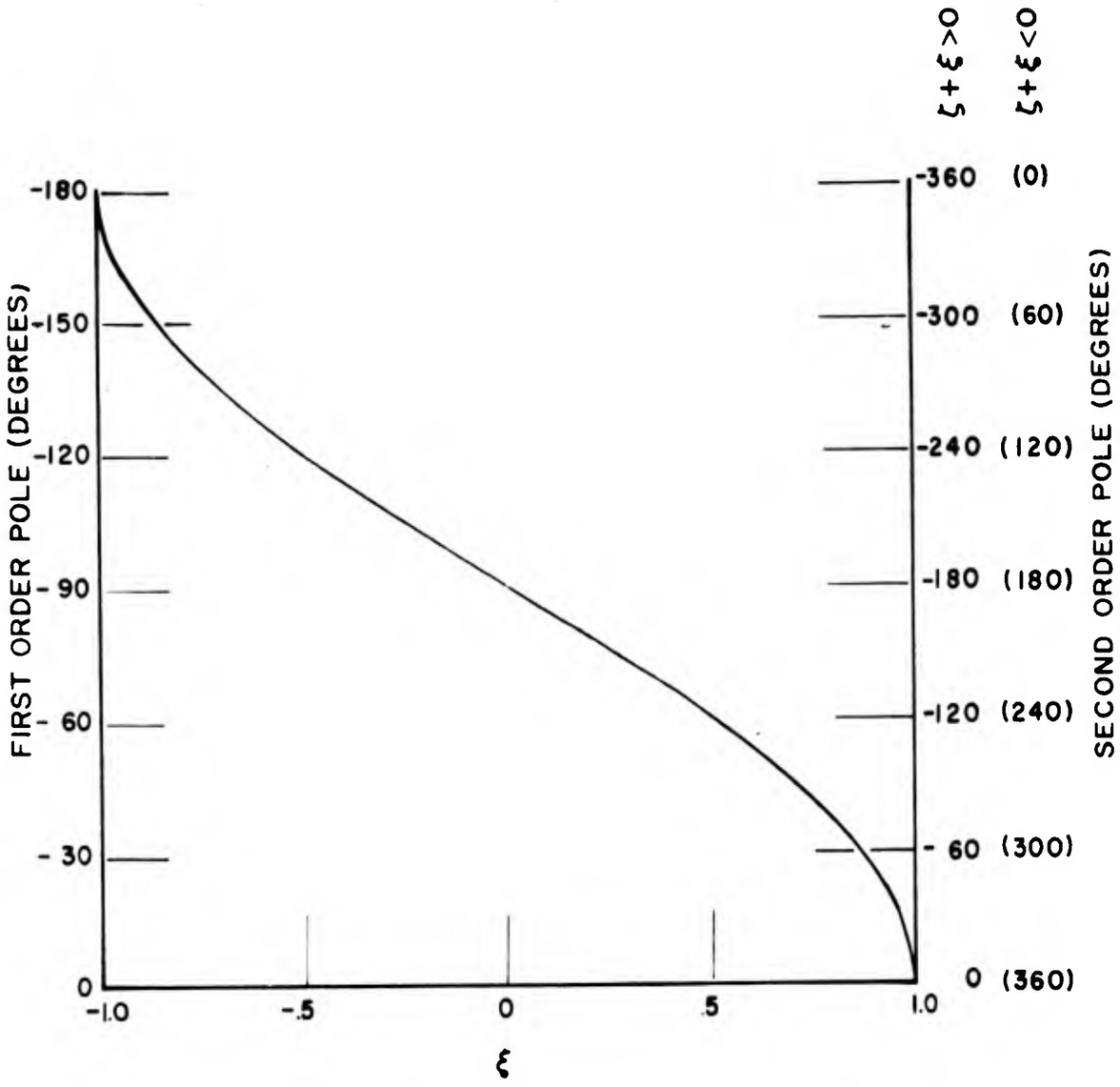

Fig. 10. High Frequency Phase Asymptotes of $G(\lambda) = \frac{1}{\lambda + 1}$, $G(\lambda) = \frac{1}{\lambda^2 + 2\zeta\lambda + 1}$

both the slope and break point locations depend upon ξ. For second order factors the break points are also a function of the damping ratio, ζ. As an aid in construction Fig. 10 presents the values of the high "frequency" phase asymptote as a function of ξ. Also, Fig. 11 gives the break points, for selected families of ξ, as a function of damping ratio.

For some purposes asymptote plots alone provide adequate approximations to the transfer function being studied. For detailed calculations, however, a more accurate representation may be needed. Templates of the actual phase and amplitude ratio functions are often used for this purpose in constructing $G(j\omega)$ and $G(\pm\sigma)$ curves, although a very large number would be required to provide a reasonable kit for other ξ values. Ordinarily, however, accurate G(s) curves for values of ξ other than zero and ± 1 are needed in only a very restricted "frequency" range. Accordingly, the use of departure corrections is probably the simplest approach. Phase and amplitude ratio departures for first and second order terms are given in Figs. 12 and 13.

C. CALCULATION OF CLOSED-LOOP ROOTS USING G(s) BODE PLOTS (References 5, 6, 18)

The roots of the closed-loop characteristic equation $1 + G(s) = 0$ can be found readily from open-loop G(s) Bode plots by determining the conditions for which $G(s) = -1$. The criteria for roots are thus identical to those given by Eq. (9) and (10). Connecting the two types of transfer function representation, Eq. (1) and (22), the "Bode gain constant," K, is related to the "root locus gain constant," κ, by

$$\kappa = K \frac{b_{m+n}}{a_n} \tag{24}$$

when a_n and b_{m+n} are nonzero. If free s terms exist in G(s) either a_n or b_{m+n} will be zero. In this circumstance the zero coefficient is replaced by the highest a_j or b_i from Eq. (1) which is nonzero. For the construction of G(s) plots the value of K is always taken as positive (a negative sign, if present in the physical gain, is reflected into the phase plot), so the angle criterion for a root, corresponding to Eq. (12), is

$$\angle G(s) = \begin{cases} (2k+1)\pi \; ; \; \dfrac{b_{m+n}}{a_n} \text{ positive} \\ 2k\pi \quad ; \; \dfrac{b_{m+n}}{a_n} \text{ negative} \end{cases} \tag{25}$$

Eq. (10) requires no further interpretation for the magnitude criterion except to note that, in db measure, Eq. (10) becomes

$$20 \log |G(s)| = |G(s)|_{db} = 0 \tag{26}$$

Using these conditions closed-loop quadratic factors which have a damping ratio of $-\xi$ will have undamped natural frequencies given by those values of μ for which $\angle G(\xi,\mu)$ will satisfy Eq. (25). The gain values compatible with a given root are established by recognizing that the zero db line must pass through the amplitude ratio curve at the values of μ consistent with satisfaction of the phase criterion.

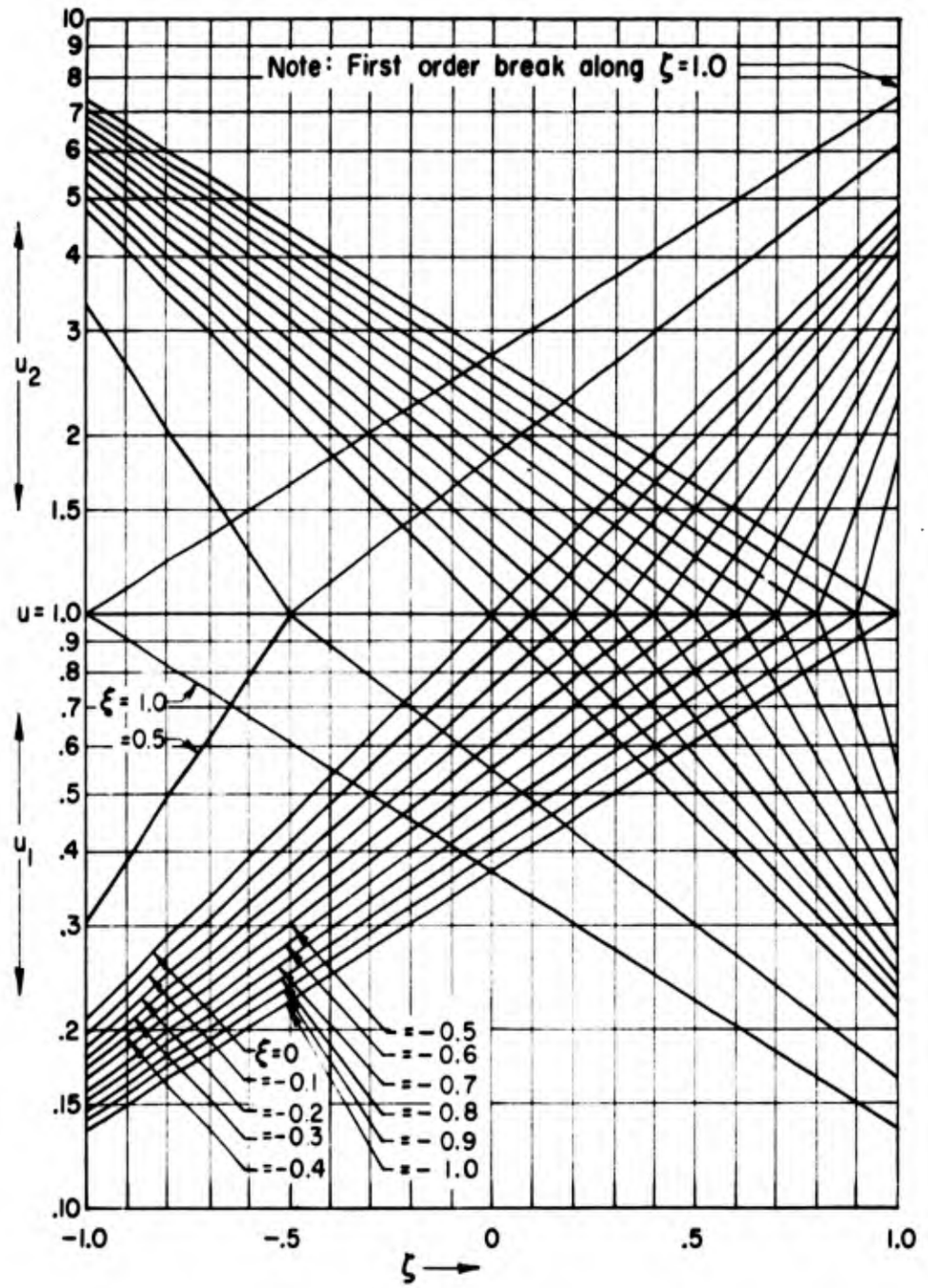

Fig. 11. Phase Break Frequencies of $G(\lambda) = \frac{1}{\lambda + 1}$, $G(\lambda) = \frac{1}{\lambda^2 + 2\zeta\lambda + 1}$

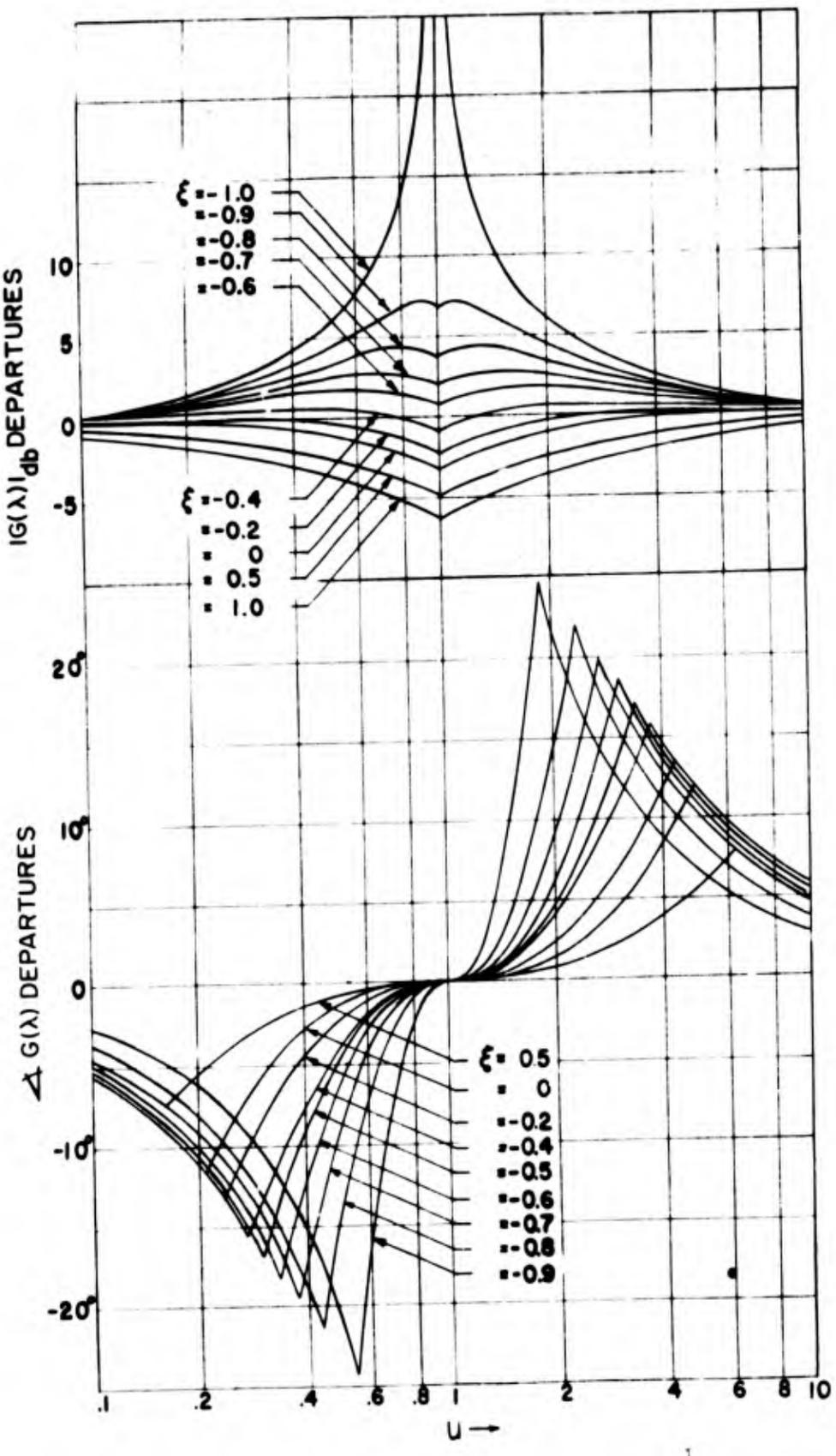

Fig. 12. Departures from Asymptotes of $G(\lambda) = \frac{1}{\lambda + 1}$

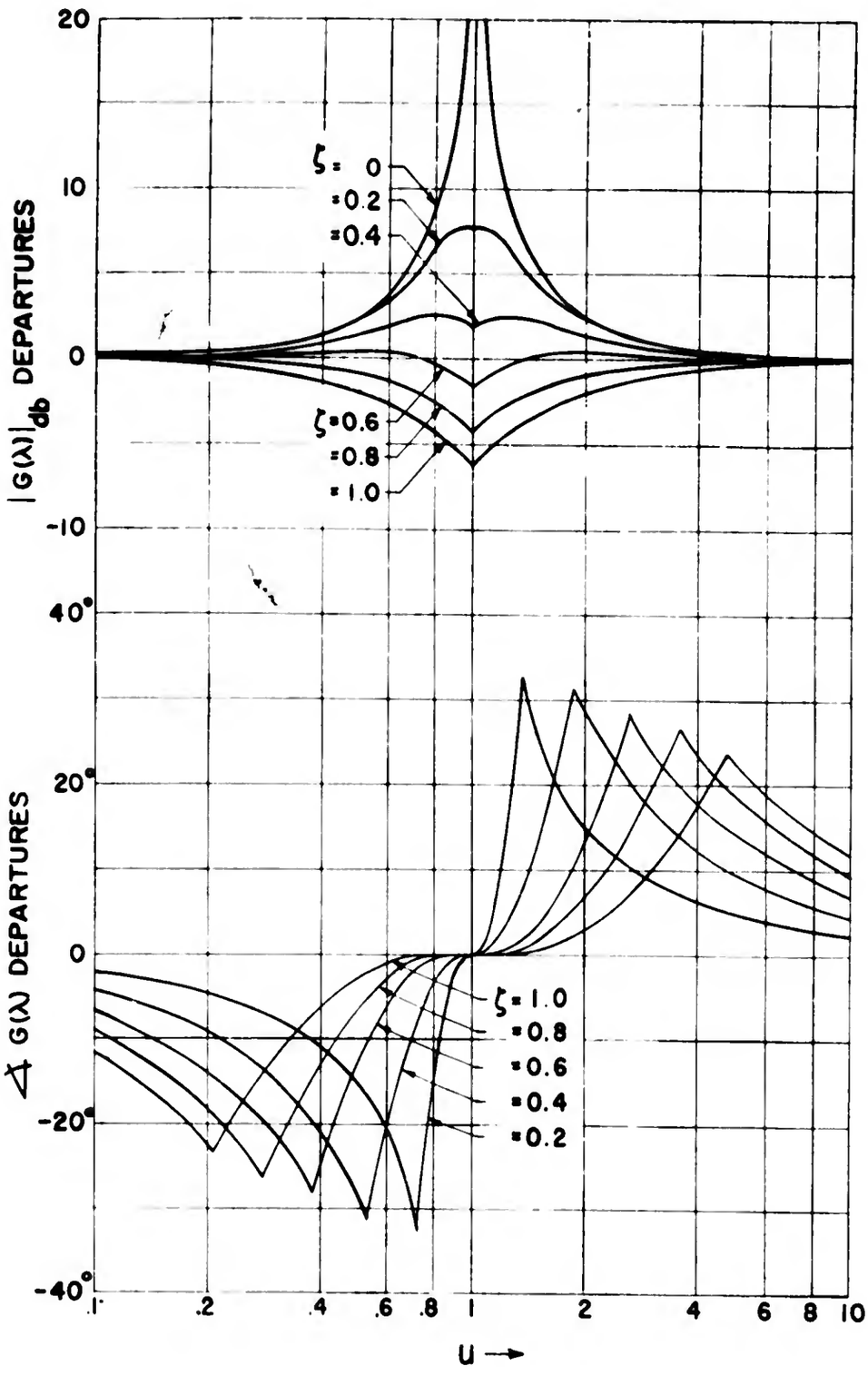

Fig. 13a. Departures from Asymptotes of $G(\lambda) = \frac{1}{\lambda^2 + 2\zeta\lambda + 1}$, $\zeta = 0$

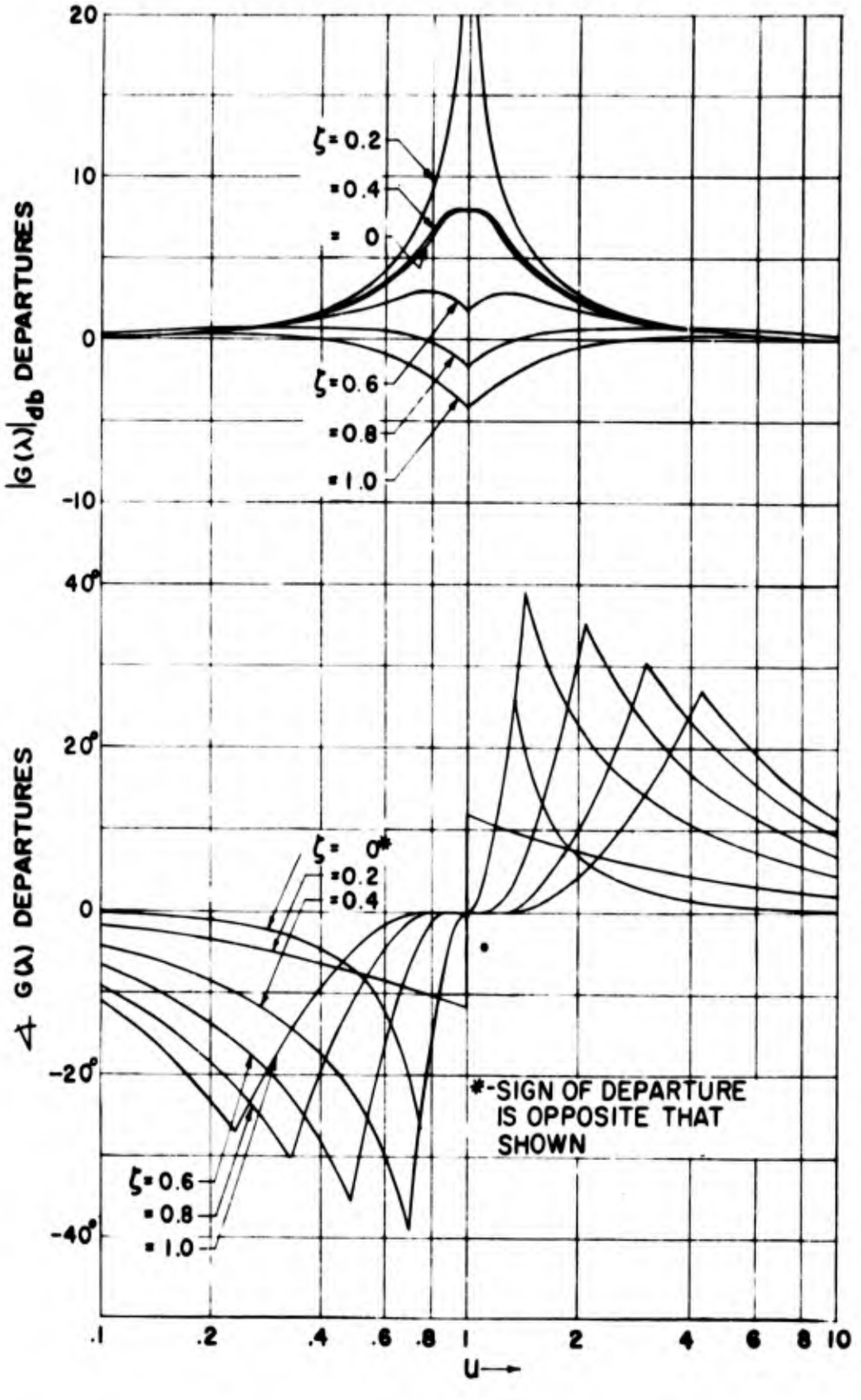

Fig. 13b. Departures from Asymptotes for $G(\lambda) = \frac{1}{\lambda^2 + 2\zeta\lambda + 1}$, $\xi = -0.2$

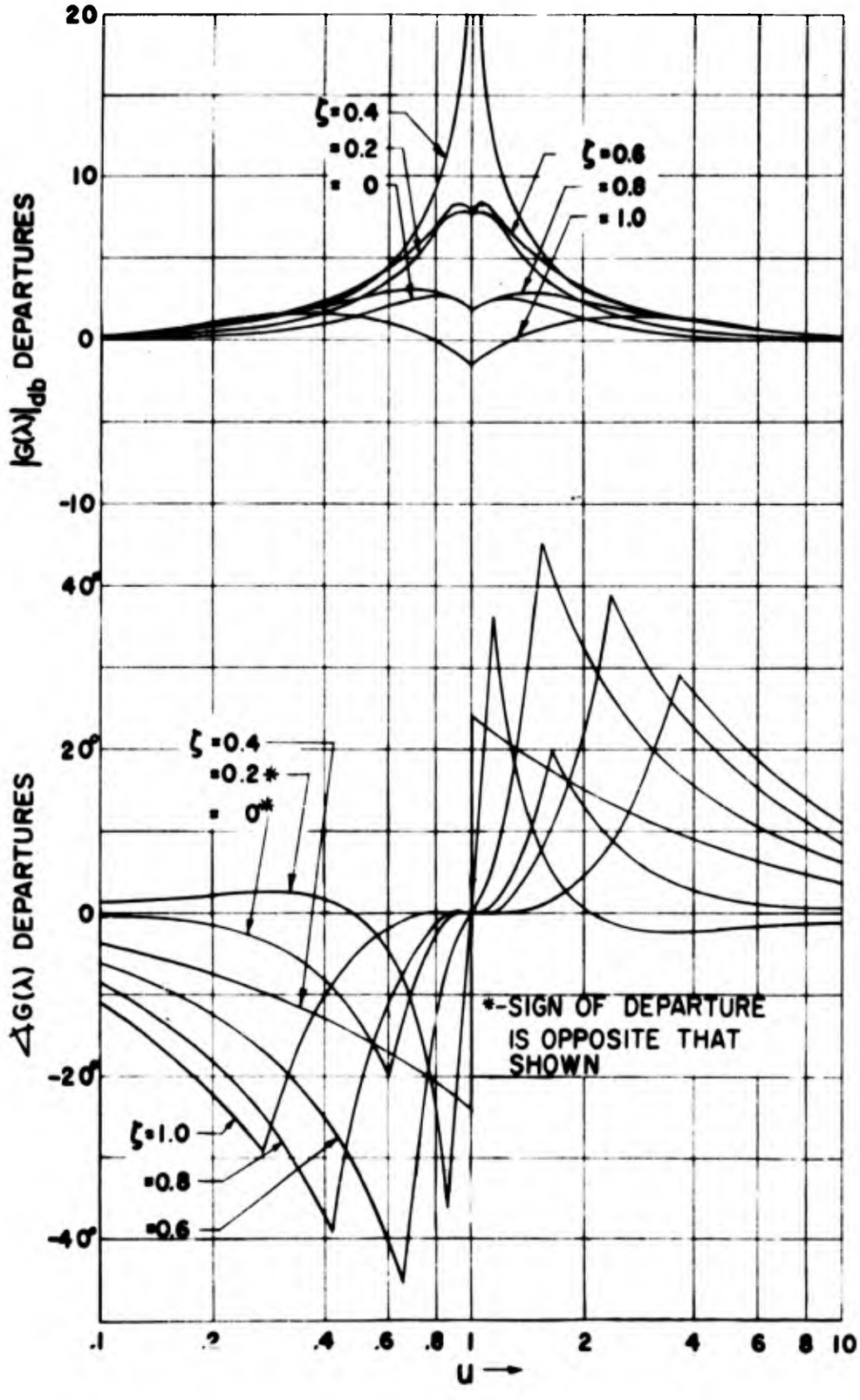

Fig. 13c. Departures from Asymptotes of $G(\lambda) = \frac{1}{\lambda^2 + 2\xi\lambda + 1}$, $\xi = -0.4$

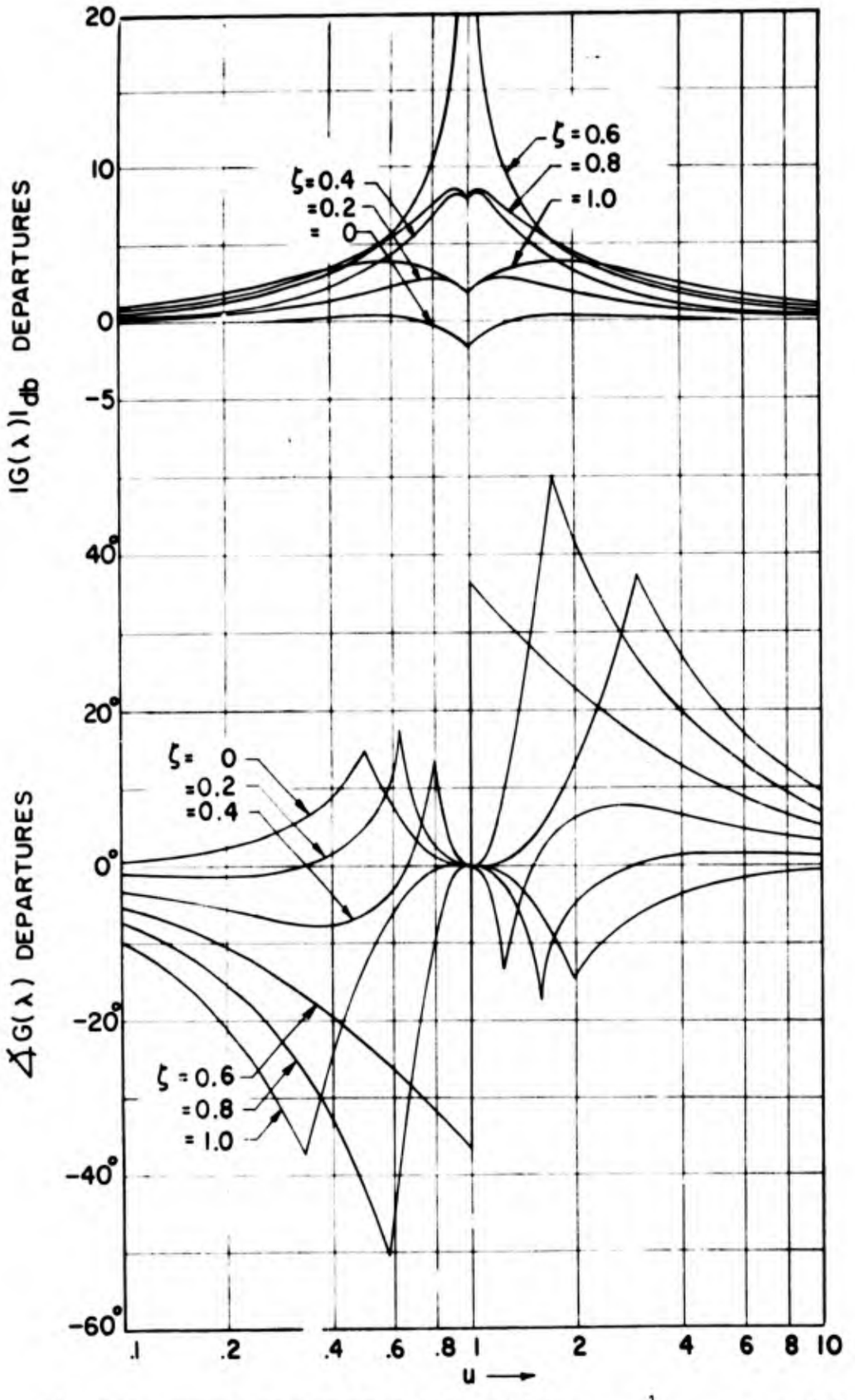

Fig. 13d. Departures from Asymptotes of $G(\lambda) = \frac{1}{\lambda^2 + 2\zeta\lambda + 1}$, $\zeta = -0.6$

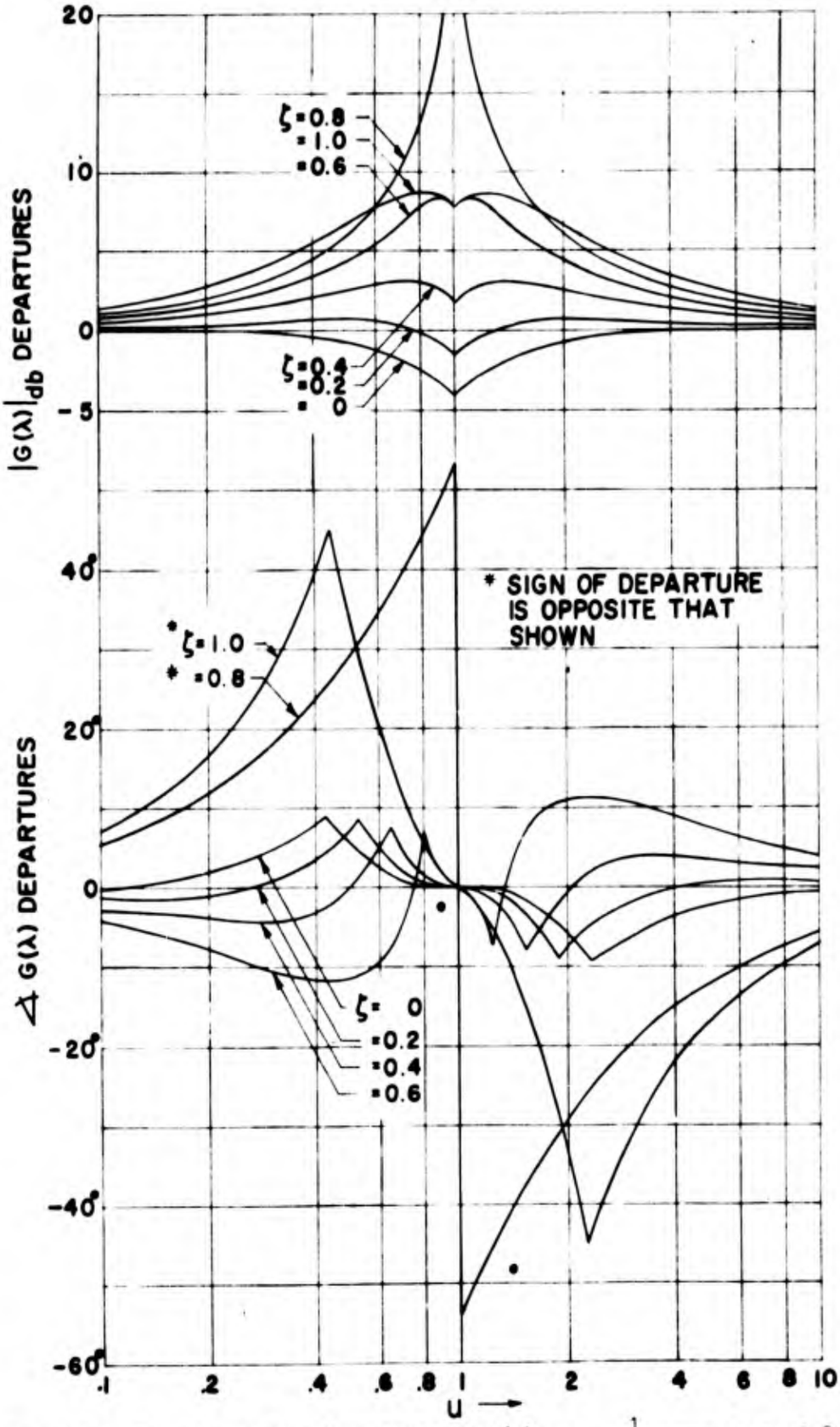

Fig. 13e. Departures from Asymptotes of $G(\lambda) = \frac{1}{\lambda^2 + 2\zeta\lambda + 1}$, $\zeta = -0.8$

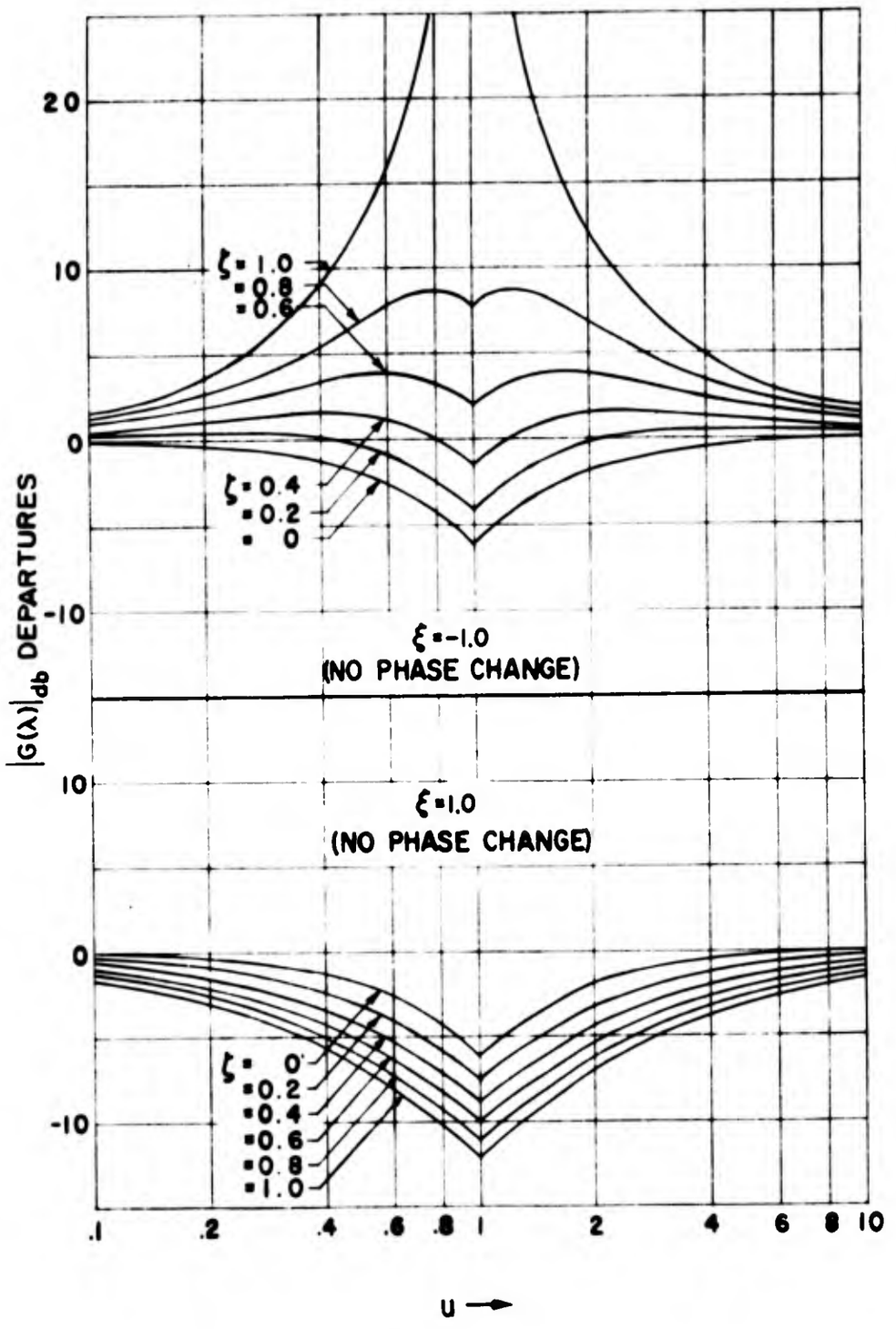

Fig. 13f. Departures from Asymptotes for $G(\lambda) = \frac{1}{\lambda^2 + 2\zeta\lambda + 1}$, $\xi = \pm 1.0$

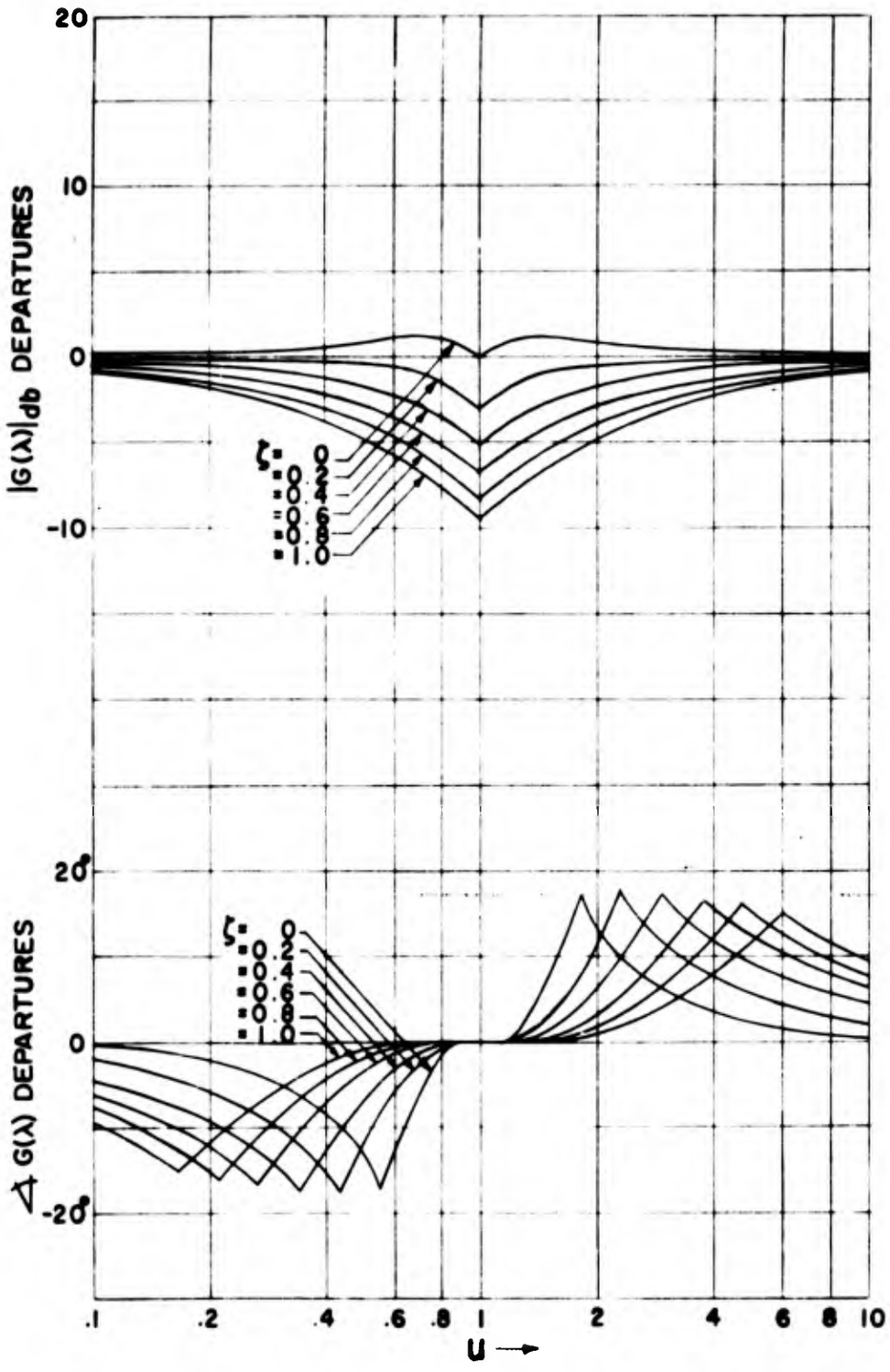

Fig. 13g. Departures from Asymptotes for $G(\lambda) = \frac{1}{\lambda^2 + 2\zeta\lambda + 1}$, $\xi = 0.5$

The use of the various G(s) Bode plots to obtain closed-loop roots is illustrated in Fig. 14 for an elementary third order system where

$$G(s) = \frac{K}{s(s+1)(\frac{s}{5}+1)}$$

The root locus for this system is that shown in Fig. 5 with a = 1, b = 5, and $\kappa = 5K$. The trends and results developed below can therefore be readily compared with those obtained from the conventional root-locus approach. Fig. 14 presents complete G(s) Bode plots for $s = j\omega$, $s = -\sigma$, and $s = (\xi + j\sqrt{1-\xi^2})\mu$ with $\xi = -0.7$. Asymptotic plots for $\xi = -0.2$, -0.9, and $+0.5$ are also given, with short segments of the actual G(s) functions in the region about $\angle G(s) = -180^\circ$ constructed from the departures of Fig. 12.

It will be noted immediately that the phase curve $\angle G(s)$ for $s = -\sigma$ has two "frequency" regions ($0 \leq \sigma \leq 1$ and $5 \leq \sigma$) where the phase is -180°. Accordingly real closed-loop inverse time constants will be present anywhere in these regions where the magnitude criterion is satisfied. For low gains (e.g., the 1-1, zero db line) the closed-loop transfer function contains three first order factors. As gain is increased two of these roots come together to form a critically damped pair where the zero db line (c-c) is just tangent to the $|G(-\sigma)|_{db}$ curve. These three branches of the $G(-\sigma)$ db amplitude ratio plot correspond directly with the real axis roots on the root locus of Fig. 5 (branches 1, 2, and 3 indicated on both Fig. 5 and Fig. 14). The point ($\sigma = 0.473$) where the line c-c is tangent to the amplitude ratio is, of course, equivalent to the real axis breakaway on the root locus. At higher gain values (zero db line below c-c) only the higher frequency branch continues to indicate the presence of a real closed-loop root. From this discussion it is apparent that the $G(-\sigma)$ Bode diagram (sometimes called a "Siggy Plot") is not only an open-loop transfer function plot for $s = -\sigma$, but is also a root-locus diagram which presents the negatives of all the real closed-loop roots as a function of open-loop gain.

For pure imaginary roots ($\xi = 0$, $\mu = \omega$) the $\angle G(j\omega)$ plot must have a phase angle of -180°. This occurs at a frequency of 2.24 rad/sec. The gain (zero db line i-i) is 15.6 db, or K = 6, and $\kappa = 30$. This neutral stability condition reflects onto the root locus as the imaginary axis crossover points.

The closed-loop complex factors with damping ratios equal to 0.2, 0.7, and 0.9 are found from the G(s) plots for $\xi = -0.2$, -0.7, and -0.9, respectively, in precisely the same fashion as used for the imaginary roots. Joining the several points where $|G(s)|$ is unity when $\angle G(s)$ is -180° results in a locus, versus gain, of the undamped natural frequencies for the closed-loop complex factors (Fig. 15). This locus also has its counterpart in the complex branch of the root locus in Fig. 5. Fig. 15, however, gives closed-loop undamped natural frequencies versus gain with damping ratio as a parameter along the locus, while the root locus portrays damping ratios and undamped natural frequencies (in polar coordinates), or dampings and damped natural frequencies (in rectangular coordinates), with gain as a parameter along the locus.

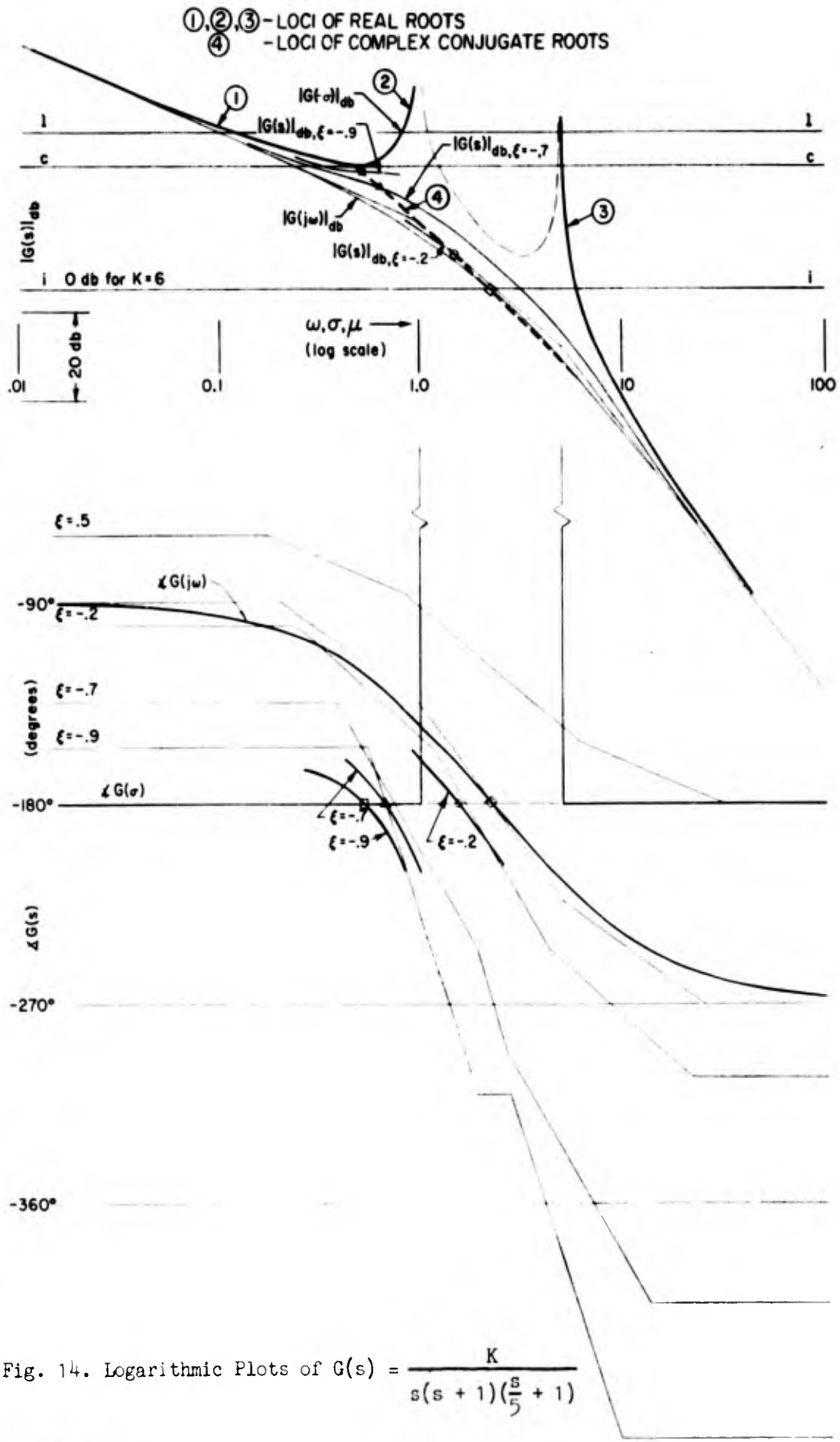

Fig. 14. Logarithmic Plots of $G(s) = \dfrac{K}{s(s+1)(\frac{s}{5}+1)}$

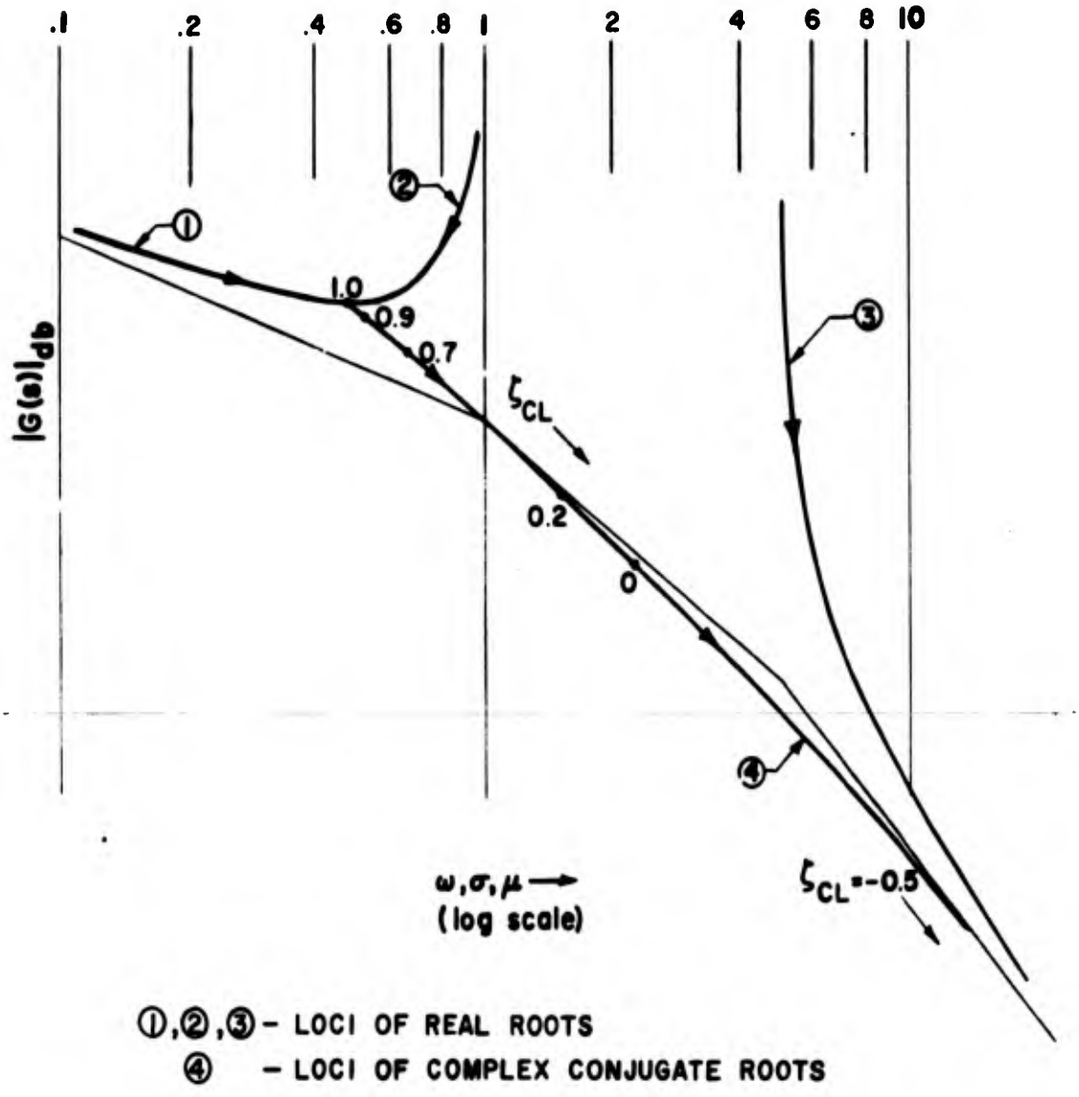

Fig. 15. Locus of Closed-Loop Transfer Function Inverse Time Constants and Undamped Natural Frequency for $G(s) = \dfrac{K}{s(s+1)(\frac{s}{5}+1)}$

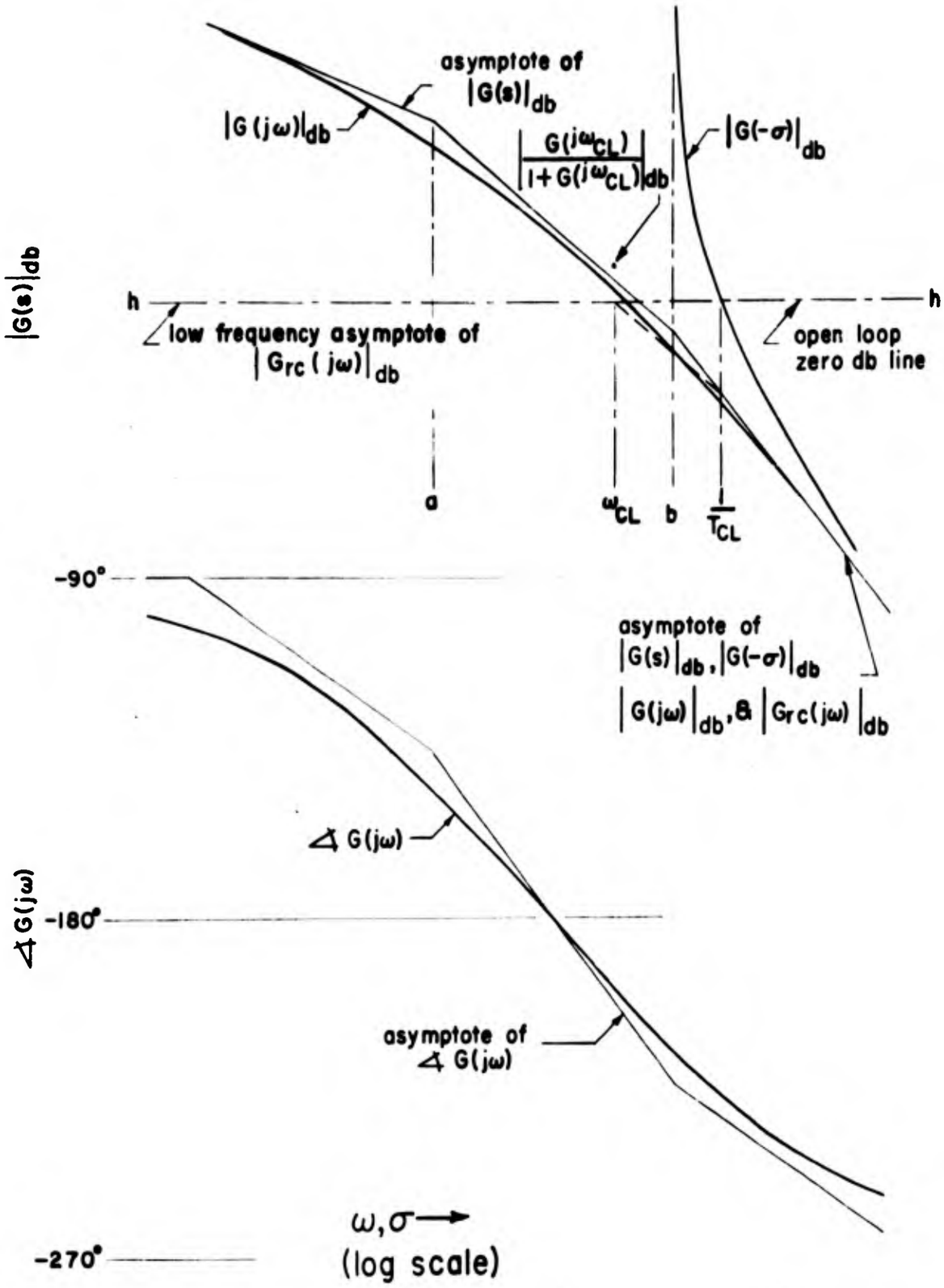

Fig. 16. Establishment of Asymptotic Plot for Closed-Loop System when

$$G(s) = \frac{K}{s(\frac{s}{a} + 1)(\frac{s}{b} + 1)}$$

Finally it will be noted that the asymptotic phase plot on Fig. 14 for $\zeta = 0.5$ does not cross the -180° phase angle line although the two lines do become tangent at very high frequencies. This indicates that, as μ approaches infinity, the damping ratio of the now unstable closed-loop quadratic factor becomes essentially constant with a value of -0.5. This behavior is reflected on the root locus by the high gain asymptotes at $\pm 60^\circ$.

D. CALCULATION OF CLOSED-LOOP ROOTS BY DECOMPOSITION

The use of generalized G(s) plots as illustrated above provides a technique which, like the root-locus method, can be a complete and separate process. The solution of many problems, however, can be accomplished much more rapidly by using only the two simplest G(s) logarithmic plots, $G(j\omega)$ and $G(-\sigma)$, to construct closed-loop G(s) diagrams which are decomposed into their constituent factors. The decomposition process, fundamentally, involves the establishment of asymptotic plots for the closed-loop system and the calculation of a few departures. The same type of procedure is widely used to extract transfer function constants from frequency response data.

The third order system can again serve as an illustrative example. Fig. 16 presents a complete $G(j\omega)$ plot and the high frequency branch of the $G(-\sigma)$ diagram. The line h-h is the open-loop zero db line corresponding to the gain at which the closed-loop characteristics are to be investigated. Since a free s exists in the denominator of G(s), this open-loop zero db line is also the low frequency asymptote of the closed-loop db amplitude ratio $|G_{rc}(j\omega)|_{db}$ (see Table I). The high frequency asymptote of $|G_{rc}(j\omega)|_{db}$ is the same as that for the open-loop db amplitude ratio $|G(j\omega)|_{db}$.

To determine the complete closed-loop asymptotic amplitude ratio,

1. Proceed up the high frequency asymptote to the point $1/T_{CL}$, which is the break frequency due to the closed-loop real root determined from the $G(-\sigma)$ plot. The midfrequency closed-loop asymptote (the dashed line) is then constructed through $1/T_{CL}$, with a slope change of +20 db/decade from that of the high frequency asymptote.

2. The intersection of the midfrequency and low frequency closed-loop db amplitude ratio asymptotes occurs at ω_{CL}, which is the undamped natural frequency of the closed-loop quadratic.

Two ($1/T_{CL}$ and ω_{CL}) of the closed-loop parameters have now been determined. The third parameter, ζ_{CL}, can be found in several ways, as listed below.

1. By direct calculation from Eq. (5), $\zeta_{CL} = \frac{1}{2\omega_{CL}}\left(b_1 - \frac{1}{T_{CL}}\right)$, where $b_1 = a + b$. It should be noted that Eq. (5) or (6) and Eq. (7) can always yield the values of the last unknown quadratic closed-loop pair in a decomposition process. In the present, almost trivial, example this last pair is also the only one present. ω_{CL} could have been found using Eq. (7), i.e.,

$$\omega_{CL} = \sqrt{Ka_nT_{CL}} = \sqrt{KT_{CL}}$$
$$= \sqrt{KabT_{CL}}$$

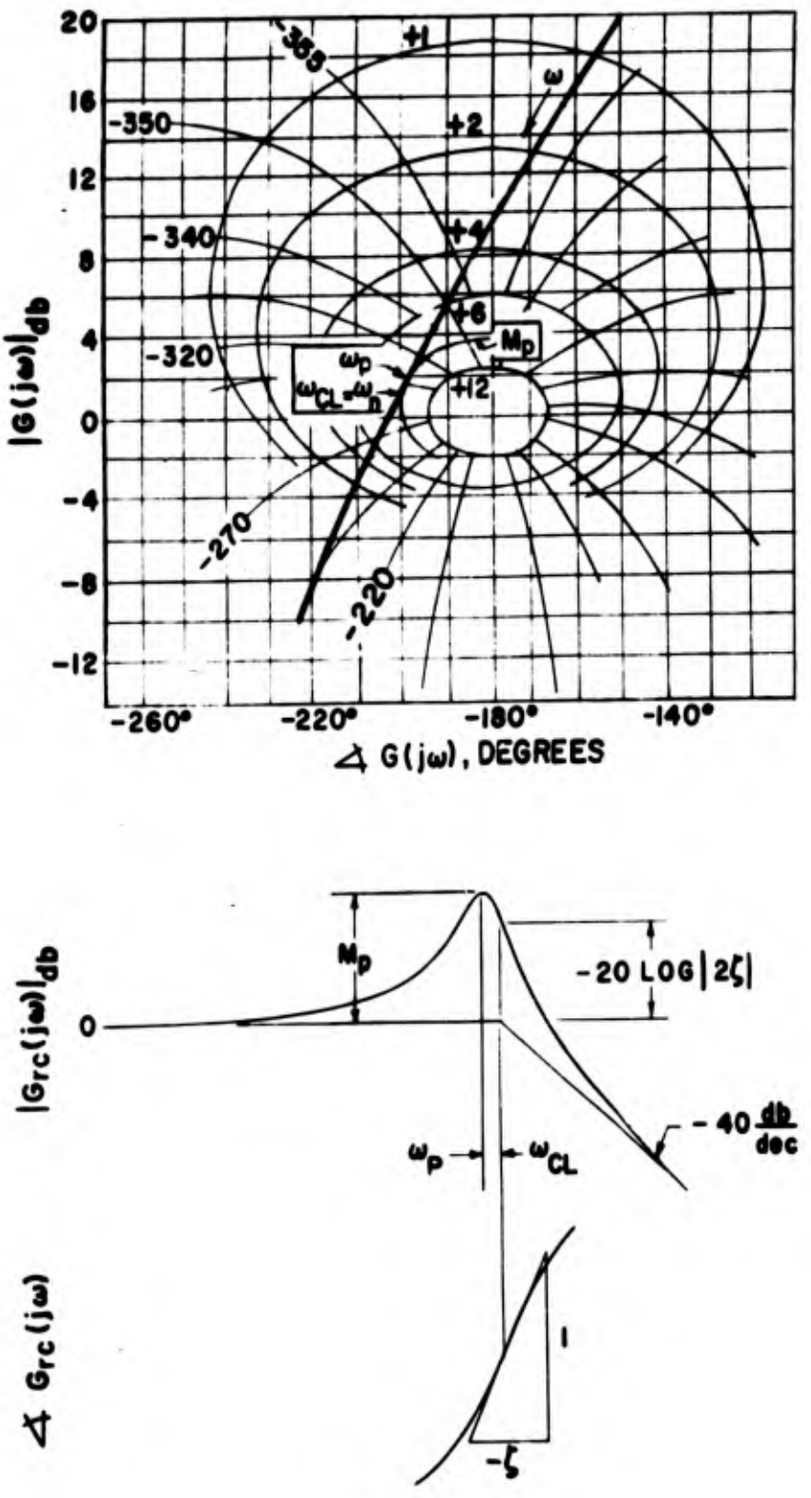

Fig. 17. Determination of Closed-Loop Parameters with the Aid of the Nichols Chart

2. Using either direct calculation, or a graphical aid (e.g., the Nichols chart (Reference 3)) find $|G(j\omega_{CL})/[1 + G(j\omega_{CL})]|$, which is the total departure of the closed-loop $|G_{rc}(j\omega)|$ transfer function from the second order break point at ω_{CL}. The component of this total departure due to the closed-loop second order factor is found by subtracting the departure, at ω_{CL}, reflected from $1/T_{CL}$. The resulting net departure is $-20 \log |2\zeta_{CL}|$.

3. Using the Nichols chart, construct $|G_{rc}(j\omega)|_{db}$ over a small range about ω_{CL} (Fig. 17). After any departure effects due to $1/T_{CL}$ are removed, the peak of the amplitude ratio plot is used to enter Fig. 18 to give the value for $|\zeta_{CL}|$. If ω_{CL} had not already been determined, and only the actual $|G_{rc}(j\omega)|_{db}$ plot was available, then an estimate for ω_{CL} could also have been obtained from the $|\zeta_{CL}|$ estimate and the determination of the ω value for which $|G_{rc}(j\omega)|_{db}$ was a maximum by using Fig. 19. Again any residual effects of other poles and zeros must be removed.

4. Using the Nichols chart, construct $\angle G_{rc}(j\omega)$ over a small range about ω_{CL} (Fig. 17). Then, if other poles and zeros are well removed from ω_{CL}, the value of ζ_{CL} can be found directly from the slope of the phase curve taken at ω_{CL}. While this procedure can be quite inaccurate, the sign of ζ_{CL} is readily assessed simply by observing the local direction of the phase slope about ω_{CL}. This fact can be used to supplement the magnitude data for ζ_{CL} found in 2 or 3 above. In most instances, of course, the sign of ζ_{CL} is readily inferred from the open-loop plots, the use of stability criteria, etc.

It should be apparent from this simple example that the decomposition process for more complex systems can often be performed extremely rapidly. The techniques to be utilized for a given problem can be drawn not only from those illustrated above, but also from the considerable number of approximations discussed in the section on directly available closed-loop data. Essential features of the process are a thorough knowledge of all the properties of first and second order factors, the various approximations, and a grasp of the possibilities implicit in going from open- to closed-loop poles and zeros. Unlike the rigid and complete disciplines of the root-locus method and its equivalent using G(s) logarithmic plots, proper application of the decomposition method requires flexibility and ingenuity which are heightened by experience. Ease of application varies with the type of problem. The illustrative system, for instance, can be solved very easily using only the high frequency branch of the $G(-\sigma)$ plot and the direct calculation for ζ_{CL} and ω_{CL}; other problems involving several second order poles or zeros which are close together can be practically impossible to decompose completely.

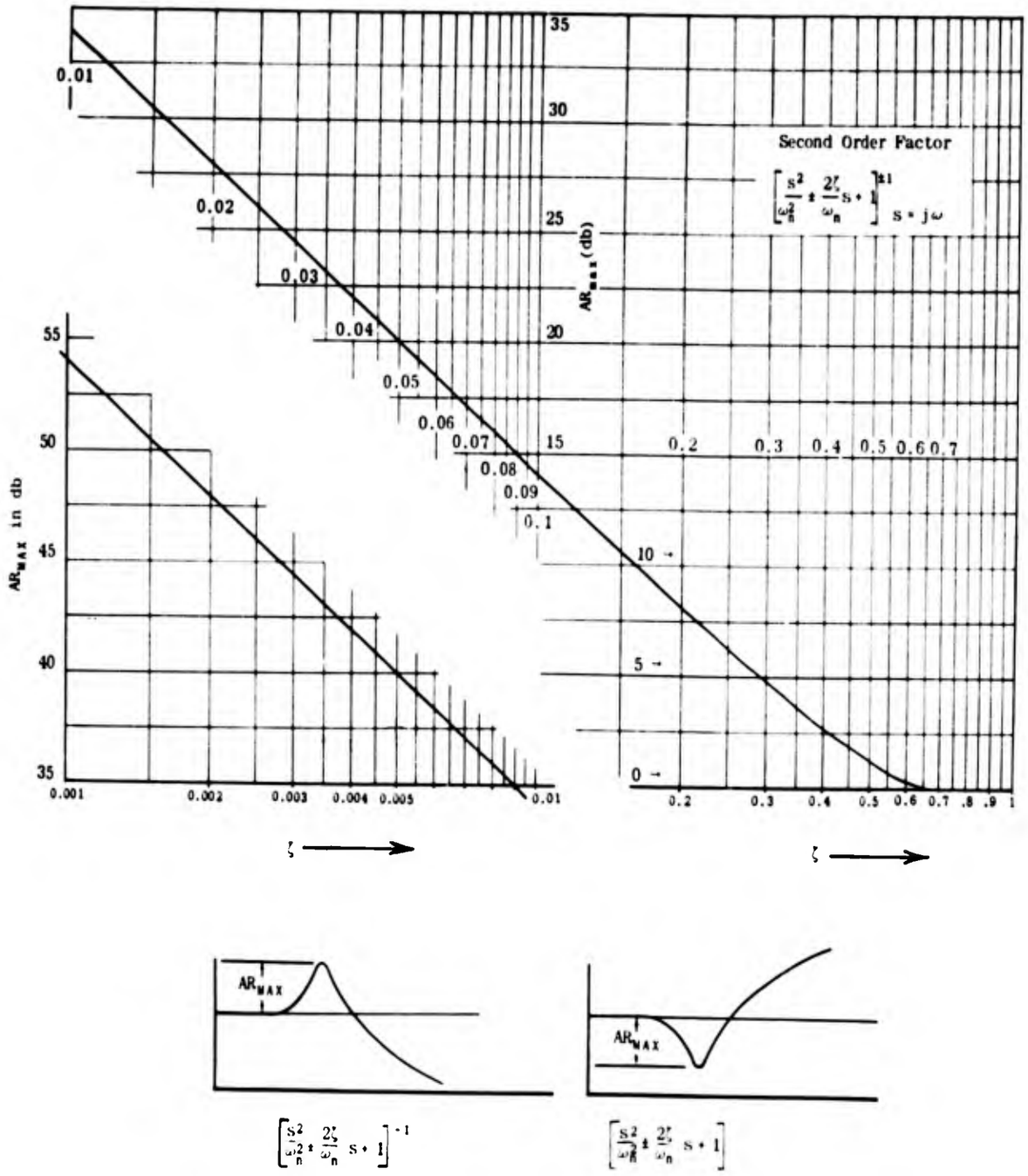

Second Order Factor

$$\left[\frac{s^2}{\omega_n^2} \pm \frac{2\zeta}{\omega_n} s + 1\right]^{\pm 1}$$

$s = j\omega$

Fig. 18. Determination of ζ from Amplitude Ratio Peak

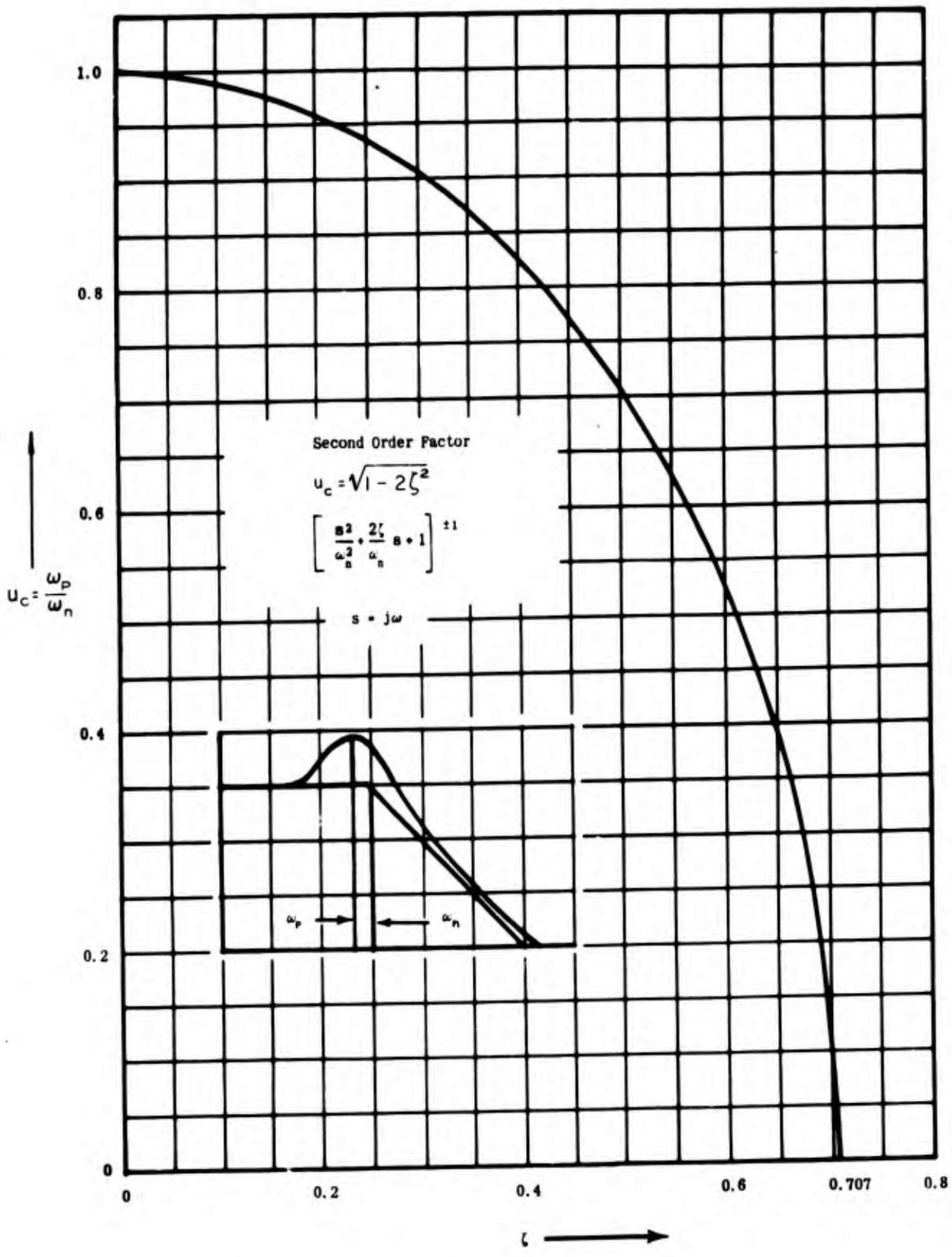

Fig. 19. Frequency at Which AR_{MAX} Occurs

SECTION V

CONNECTIONS BETWEEN THE METHODS

In the previous sections the problem of finding closed-loop roots by operations upon graphical forms of the open-loop transfer function has considered G(s) logarithmic and pole-zero plots separately. Techniques based upon either representation have been summarized, and examples have demonstrated their use in determining the closed-loop roots. Although some connection between the two general graphical forms has been implicit in the discussion, an explanation of the explicit relationships has been deferred to this point. The subsequent discussion will cover two types of interrelationships—theoretical and practical.

At the theoretical level the various forms of the open-loop transfer function have a common bond in the realm of potential theory. G(s) may be expressed as

$$G(s) = G(\sigma + j\omega) = |G(\sigma,\omega)|\, e^{j\varphi(\sigma,\omega)} = U(\sigma,\omega) + jV(\sigma,\omega) \tag{27}$$

where

$$|G(\sigma,\omega)|^2 = U^2(\sigma,\omega) + V^2(\sigma,\omega)$$

$$\varphi(\sigma,\omega) = \tan^{-1}\frac{V(\sigma,\omega)}{U(\sigma,\omega)}$$

and ln G(s) is given by

$$\ln G(s) = \ln |G(\sigma,\omega)| + j\varphi(\sigma,\omega) \tag{28}$$

G(s) is an analytic function for all values of s except those which correspond to poles and zeros. Consequently G(s) and ln G(s), or their constituent elements in Eq. (27) and (28), will obey Laplace's equation in the two variables σ and ω in all regions of the s-plane devoid of singularities. Thus

$$\begin{aligned}
\nabla^2 |G(\sigma,\omega)| &= \frac{\partial^2 |G(\sigma,\omega)|}{\partial\sigma^2} + \frac{\partial^2 |G(\sigma,\omega)|}{\partial\omega^2} = 0 \\
\nabla^2 U(\sigma,\omega) &= 0 \\
\nabla^2 V(\sigma,\omega) &= 0 \\
\nabla^2 \ln |G(\sigma,\omega)| &= 0 \\
\nabla^2 \varphi(\sigma,\omega) &= 0
\end{aligned} \tag{29}$$

The fact that Laplace's equation also describes a wide variety of physical phenomena suggests that physical analogies be used to help delineate the connections between the various forms of transfer function representations (References 14, 19-22).

As one such analogy (Reference 20), consider the s-plane as an infinite sheet of uniformly conducting resistive material. The open-loop poles and zeros can then be represented as point sources and sinks of current, placed at the pole and zero locations, with strength proportional to the order of the pole or zero. At any point, s, on the sheet the potential $\Phi(s)$, measured with respect to the potential $\Phi(s_o)$ existing at some reference point s_o, will be

$$\Phi(s) \quad \propto \quad \ln \frac{G(s)}{G(s_o)} \tag{30}$$

Similarly, the current, i, flowing across a path between the two points will be

$$i \propto \varphi(s) - \varphi(s_c) \tag{31}$$

so that the lines of constant current in the s-plane correspond to lines of constant phase.

Applying this analogy to the elementary third order system, the three poles would be represented as unit sources of current located at s = 0, -a, and -b, as shown in Fig. 20. This figure also shows the results which would be obtained by measuring the potential along the σ and $j\omega$ axes, and along the line $s = (\xi + j\sqrt{1 - \xi^2})\mu$. From Eq. (30) it is apparent that these potential functions are proportional to the open-loop logarithmic amplitude ratio plots for $s = \sigma$, $j\omega$ and $(-\xi + j\sqrt{1 - \xi^2})\mu$ previously shown in Fig. 14, except that the abscissa is in linear rather than logarithmic units.

Lines of constant phase, corresponding to constant current flow lines, are shown in Fig. 21. These lines, besides being phase loci,* are also loci which satisfy the angle condition for open-loop transfer functions which have the form

$$G(s)e^{-j\theta} = -1 \tag{32}$$

where θ is a constant. The $\pm 180^\circ$ and $0, \pm 360^\circ$ phase loci are conventional root loci for κ positive and negative, respectively.

An especially illuminating integration of the several graphical forms for G(s) is shown by the three-dimensional model of Fig. 22. Here the s-plane forms the base and the potential is displayed in the vertical dimension. The reference potential plane for the model is adjusted to correspond to the value of open-loop gain for instability.** The lines formed by the black wires are loci of points where G(s) = -1. These lines, therefore, are three-dimensional root

---

*For a complete discussion of phase loci see Reference 23.

**In general, the intersection of the potential surfaces with horizontal planes parallel to the reference s-plane yield the constant gain loci discussed in Reference 13.

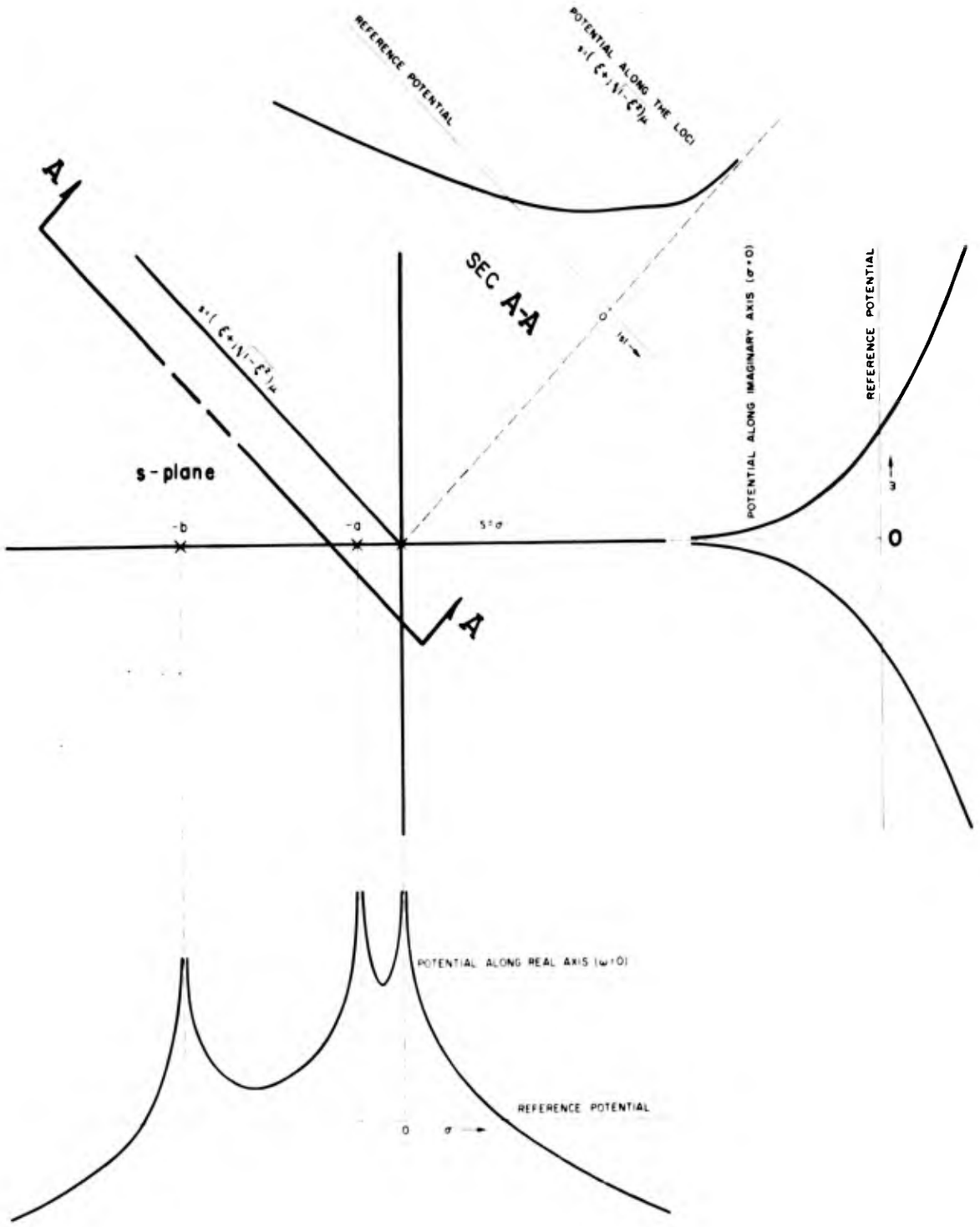

Fig. 20. Potential Surveys Along Various Lines in the s-Plane

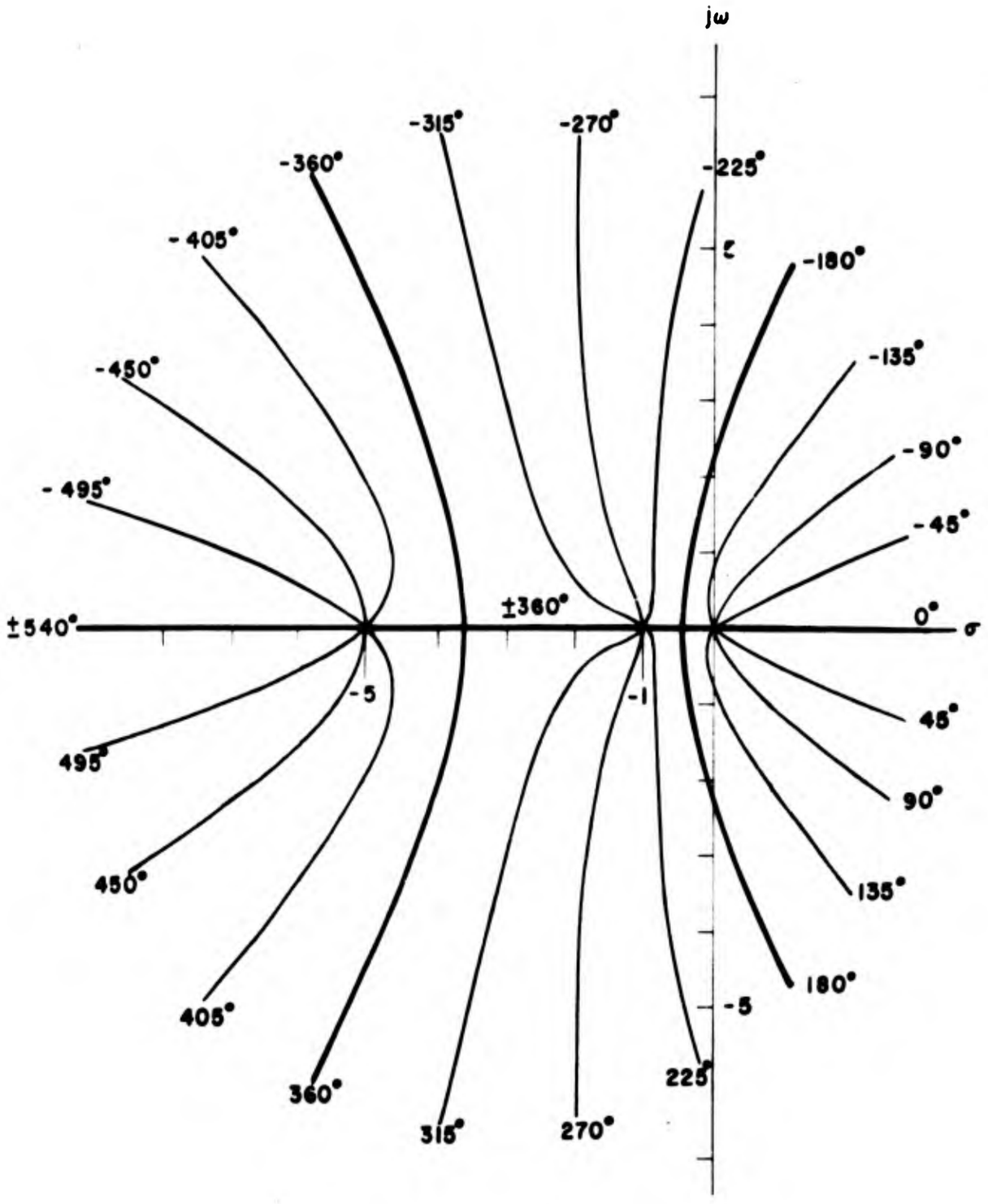

Fig. 21. Lines of Constant Phase, or Phase Angle Loci for $G(s) = \frac{K}{s(s+1)(s+5)}$

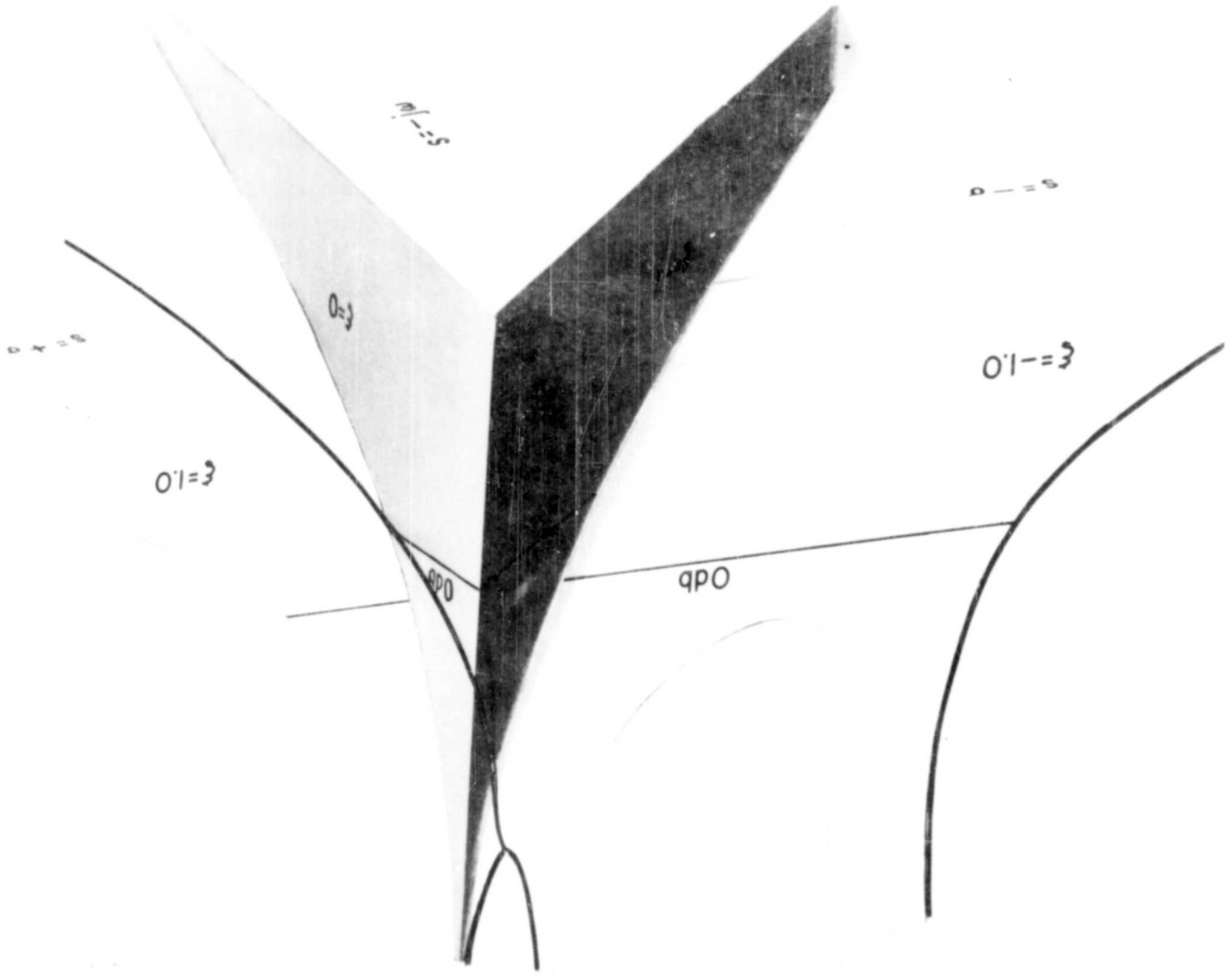

Fig. 22. Three-Dimensional Model of the Various Graphical Forms for G(s) and the Three-Dimensional Root Locus

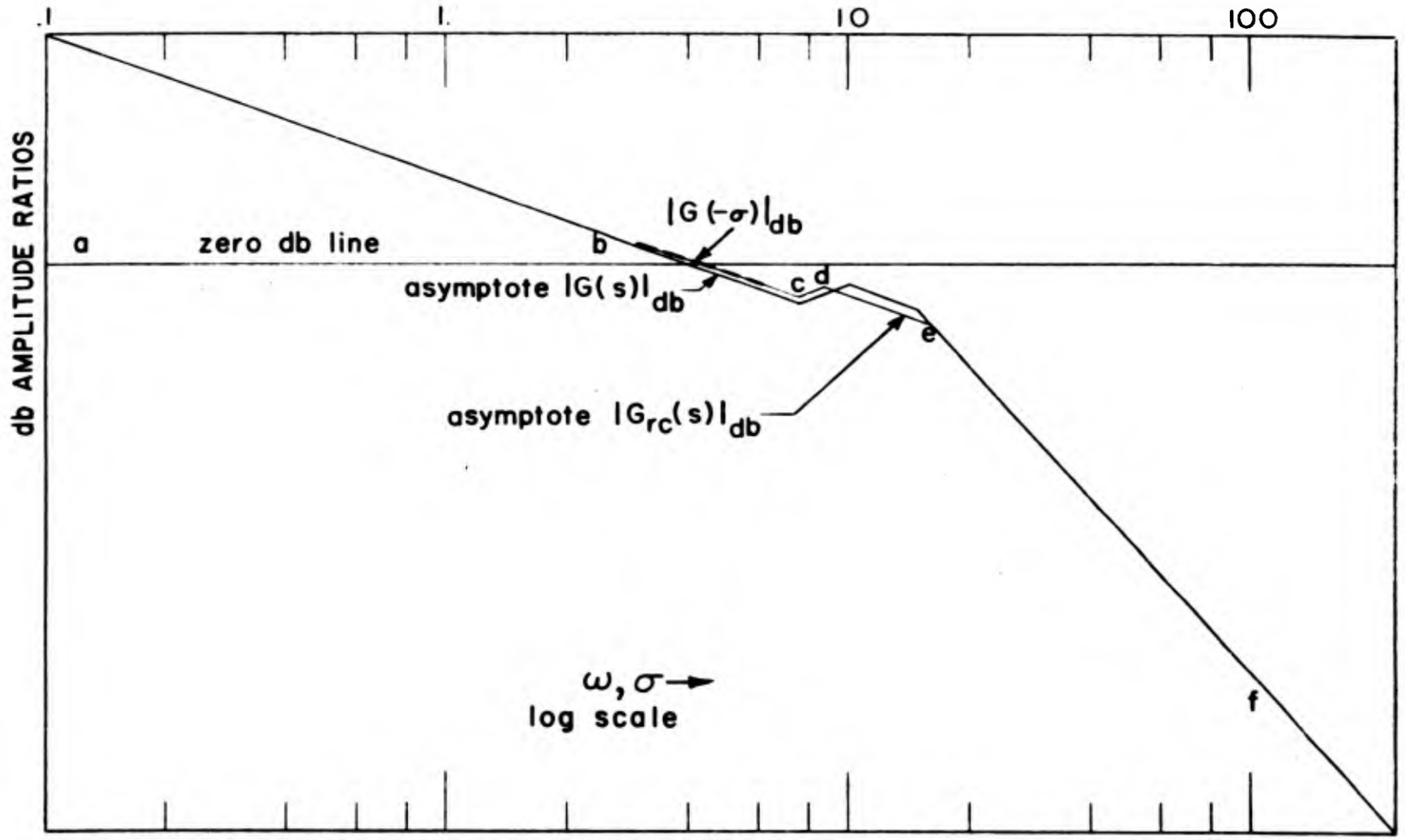

Fig. 23. Solution for Closed-Loop Roots for $G(s) = \dfrac{4\left[\left(\frac{s}{7.5}\right)^2 + \frac{2(0.1)s}{7.5} + 1\right]}{s\left[\left(\frac{s}{10}\right)^2 + \frac{2(0.1)s}{10} + 1\right]\left[\left(\frac{s}{15}\right)^2 + \frac{2(0.1)s}{15} + 1\right]}$

loci, with gain (in db) now being represented in terms of the height above the s-plane instead of as a parameter along the usual two-dimensional root locus. The conventional root locus, of course, is simply a view of the black wires from above.*

Fig. 22 illustrates nicely the complete theoretical tie which exists between the several useful forms of open-loop transfer function graphical descriptions. It now remains to consider the practical use of these same open-loop transfer function plots, or portions thereof, as elements of an integrated technique for solution of the analysis problem.

While either the G(s) logarithmic representations or the pole-zero plot can be used to find complete information about the closed-loop roots, an intermix of techniques often provides the most effective and efficient solution. Since the best combination depends upon the specifics of a given problem, an example provides the simplest way to illustrate some of the possibilities for joint use.

Consider an open-loop transfer function given by

$$G(s) = \frac{4\left[\left(\frac{s}{7.5}\right)^2 + \frac{2(0.1)s}{7.5} + 1\right]}{s\left[\left(\frac{s}{10}\right)^2 + \frac{2(0.1)s}{10} + 1\right]\left[\left(\frac{s}{15}\right)^2 + \frac{2(0.1)s}{15} + 1\right]}$$

$$= \frac{1600\left[s^2 + 2(0.1)(7.5)s + (7.5)^2\right]}{s\left[s^2 + 2(0.1)(10)s + (10)^2\right]\left[s^2 + 2(0.1)(15)s + (15)^2\right]}$$

The first step in the solution for the closed-loop roots is the construction of the asymptotic $|G(s)|_{db}$ plot (Fig. 23). The departures from the asymptote of $|G(-\sigma)|_{db}$ are then added, in the immediate region of crossover, to establish the value of the one real root, $\sigma = -4.4$. Portions of the closed-loop asymptotic plot for $|G_{rc}(s)|_{db}$ can then be found. These include:

1. The low frequency asymptote, a—b, which extends from zero to 4.4.

2. A midfrequency asymptote with a -20 db/decade slope, b—c, going from 4.4 to the frequency (7.5) of the complex zeros.

---

*Similar analogies can be made with fluid dynamic, gravitational, magnetostatic, elastic, or electrostatic potential problems. For two-dimensional irrotational flow of an incompressible fluid, for example, the poles and zeros are again sources and sinks, $\ln|G(\sigma,\omega)|$ is the potential function, and $\varphi(\sigma,\omega)$ is the stream function. Phase loci become streamlines, and the root locus is the 1/2 streamline (Reference 22).

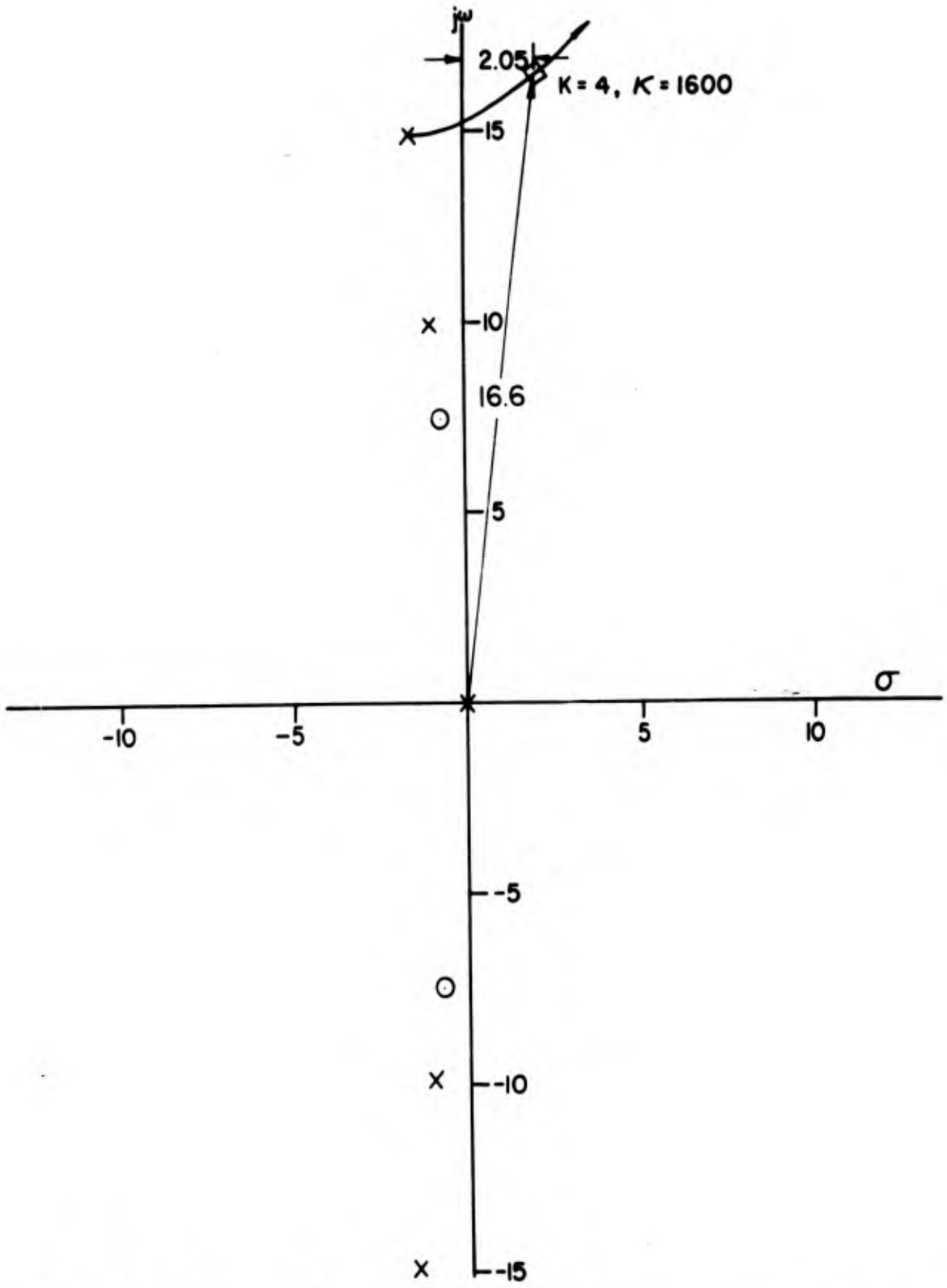

Fig. 24. High Frequency Portion of Root Locus for

$$G(s) = \frac{1600\left[s^2 + 2(0.1)(7.5)s + (7.5)^2\right]}{s\left[s^2 + 2(0.1)(10)s + (10)^2\right]\left[s^2 + 2(0.1)(15)s + (15)^2\right]}$$

3. Another midfrequency asymptote, starting at c and having a slope of +20 db/decade reflecting the +40 db/decade increment due to the complex zeros.

4. The high frequency asymptote, extending back from f with a slope of -60 db/decade.

At this stage only one closed-loop factor is known, and only one asymptote (of the two required) is available for each of the two complex pairs remaining to be found. The missing intermediate asymptote can be found by cut and try procedures using either G(s) plots or by curve fitting and decomposition. Neither is direct nor, in this case, particularly accurate. By far the simplest process is to construct one branch of the root locus, and solve for the root when $\kappa = 1600$ ($K = 4$). This is shown in Fig. 24, where the high frequency closed-loop factor is found to be $s^2 - 2(0.125)s + (16.6)^2$. The value of 16.6 for the undamped natural frequency establishes the point e on the high frequency asymptote of Fig. 23. The final intermediate asymptote is then constructed through e with a slope of -20 db/decade. Its intersection at d with the +20 db/decade asymptote from c determines the value of the final undamped natural frequency, 8.8. This undamped natural frequency can also be found using Eq. (7). The fact that all the roots must sum to -5 per Eq. (5) is used to determine a value for the last remaining damping ratio. Thus, the final result for the closed-loop transfer function is

$$G_{rc}(s) = \frac{\left[\left(\frac{s}{7.5}\right)^2 + \frac{2(0.1)s}{7.5} + 1\right]}{\left(\frac{s}{4.4} + 1\right)\left[\left(\frac{s}{8.8}\right)^2 + \frac{2(0.265)s}{8.8} + 1\right]\left[\left(\frac{s}{16.6}\right)^2 - \frac{2(0.125)s}{16.6} + 1\right]}$$

The closed-loop transfer function obtained using this integrated graphical procedure compares favorably with the more precise version,

$$G_{rc}(s) = \frac{\left[\left(\frac{s}{7.5}\right)^2 + \frac{2(0.1)s}{7.5} + 1\right]}{\left(\frac{s}{4.32} + 1\right)\left[\left(\frac{s}{8.81}\right)^2 + \frac{2(0.262)s}{8.81} + 1\right]\left[\left(\frac{s}{16.39}\right)^2 - \frac{2(0.120)s}{16.39} + 1\right]}$$

obtained by factoring the characteristic equation. The numerical differences are, of course, due solely to the graphical processes involved and are not fundamental.

This last example nicely illustrates the point that the feedback systems designer should not only have a working knowledge of all available feedback system analysis methods, but also an appreciation for the additional power offered by their use in concert. It also indicates the efficiency gained by adopting an eclectic viewpoint, and so brings this presentation of unified analysis procedures to a reasonable conclusion.

REFERENCES

1. Routh, E. J., Dynamics of a System of Rigid Bodies, Macmillan, London, 1905, Sixth Edition. Reprinted by Dover Publications, Inc., New York, N. Y., 1955, pp. 221-231.

2. Nyquist, H., Regeneration Theory, Bell System Technical Journal, vol. 11, January 1932, pp. 126-147.

3. James, H. M., N. B. Nichols, and R. S. Phillips, Theory of Servomechanisms, McGraw-Hill Book Co., Inc., New York, N. Y., 1947, pp. 67-72 and pp. 179-186.

4. Vazsonyi, A., A Generalization of Nyquist's Stability Criteria, Jour. App. Physics, vol. 20, September 1949, pp. 863-867.

5. Biernson, G., Quick Methods for Evaluating the Closed-Loop Poles of Feedback Control Systems, Trans. AIEE, vol. 72, Pt. II, 1953, pp. 53-70.

6. Basu, S. K., Rapid Determination of Approximate Closed-Loop Poles of Feedback Control Systems, Trans. AIEE, vol. 79, Pt. II, pp. 96-99.

7. Evans, W. R., Graphical Analysis of Control Systems, Trans. AIEE, vol. 67, Pt. I, 1948, pp. 547-551.

8. Evans, W. R., Control System Synthesis by Root Locus Methods, Trans. AIEE, vol. 69, Pt. I, 1950, pp. 66-69.

9. Evans, W. R., Control System Dynamics, McGraw-Hill Book Co., Inc., New York, N. Y., 1954.

10. Lass, H., A Note on the Root-Locus Method, Proc. IRE, vol. 44, May 1956, p. 693.

11. Bollay, W. E., Aerodynamic Stability and Automatic Control, Jour. IAS, vol. 18, September 1951, pp. 569-617.

12. Kulda, R. J., and D. T. McRuer, The Root Locus Method, Chapter 3, Section 4 of "Methods of Analysis and Synthesis of Piloted Aircraft Flight Control Systems," BuAer Report AE-61-4I, March 1952, pp. III-20 to III-32.

13. Yeh, V. C. M., The Study of Transients in Linear Feedback Systems by Conformal Mapping and the Root Locus Method, Trans. ASME, vol. 76, March 1954, pp. 349-361.

14. Reza, F. M., Some Mathematical Properties of Root Loci for Control System Design, Trans. AIEE, vol. 75, Pt. I, 1956, pp. 103-108.

15. Yeh, V. C. M., Synthesis of Feedback Control Systems by Gain-Contour and Root-Contour Methods, Trans. AIEE, vol. 75, Pt. II, 1956, pp. 89-95.

16. Banerjee, H., and T. J. Higgins, Root Locus Delineations for Higher-Order Servomechanisms, Proc. of the National Electronic Conf., vol. XIII, 1957, pp. 520-536.

17. Bode, H. W., Network Analysis and Feedback Amplifier Design, D. Van Nostrand Co., Inc., New York, N. Y., 1945.

18. Kusters, N. L., and W. J. M. Moore, A Generalization of the Frequency Response Method for the Study of Feed-Back Control Systems, Automatic and Manual Control, (A. Tustin, ed.) Butterworths Scientific Publications, London, 1952, pp. 105-122.

19. Daniell, P. J., Analogy Between the Interdependence of Phase-shift and Gain in a Network and the Interdependence of Potential and Current Flow in a Conducting Sheet, Ministry of Supply Servo Library, Ref. B 39, 1942.

20. Boothroyd, A. R., and J. H. Westcott, The Application of the Electrolytic Tank to Servo-mechanism Design, Automatic and Manual Control (A. Tustin, ed.) Butterworths Scientific Publications, London, 1952, pp. 87-103.

21. Fossier, M. W., and H. A. Rosen, A Field-Mapping Method for Analysis and Synthesis of Linear Closed-Loop Systems, Jour. IAS, vol. 20, March 1953, pp. 205-209.

22. Tsien, H. S., Engineering Cybernetics, McGraw-Hill Book Co., Inc., New York, N. Y., 1954, pp. 46-48.

23. Chu, Y., Synthesis of Feedback Control System by Phase-Angle Loci, Trans. AIEE, Pt. II, vol. 71, 1952, pp. 330-339.

Flight Control Laboratory, Aeronautical Systems Division, W-P Air Force Base, Ohio.

UNIFIED ANALYSIS OF LINEAR FEEDBACK SYSTEMS, by Duane T. McRuer. July 1961. 71 p. incl. illus. (Proj. 8219; Task 82162) (ASD TR 61-118) Unclassified Report

A summary is given of techniques and concepts useful in the analysis of linear feedback systems; these procedures are then correlated and integrated into a unified analysis method. The central feedback system analysis problem discussed is that of finding complete closed-loop system characteristics from a knowledge of the open-loop transfer function. Several forms of graphical

(over)

UNCLASSIFIED

UNCLASSIFIED

representation for open-loop transfer functions, including pole-zero plots and generalized G(s) logarithmic diagrams, are considered. The use of these graphical forms in generalized root-locus and decomposition techniques to find closed-loop transfer functions is illustrated with examples. The various feedback system analysis procedures are shown to have a common theoretical connection and to be supplementary techniques when used in an integrated manner to attack specific problems.

UNCLASSIFIED

Flight Control Laboratory, Aeronautical Systems Division, W-P Air Force Base, Ohio.

UNIFIED ANALYSIS OF LINEAR FEEDBACK SYSTEMS, by Duane T. McRuer. July 1961. 71 p. incl. illus. (Proj. 8219; Task 82162) (ASD TR 61-118) Unclassified Report

A summary is given of techniques and concepts useful in the analysis of linear feedback systems; these procedures are then correlated and integrated into a unified analysis method. The central feedback system analysis problem discussed is that of finding complete closed-loop system characteristics from a knowledge of the open-loop transfer function. Several forms of graphical

(over)

UNCLASSIFIED

representation for open-loop transfer functions, including pole-zero plots and generalized G(s) logarithmic diagrams, are considered. The use of these graphical forms in generalized root-locus and decomposition techniques to find closed-loop transfer functions is illustrated with examples. The various feedback system analysis procedures are shown to have a common theoretical connection and to be supplementary techniques when used in an integrated manner to attack specific problems.

UNCLASSIFIED

Flight Control Laboratory, Aeronautical Systems Division, W-P Air Force Base, Ohio.

UNIFIED ANALYSIS OF LINEAR FEEDBACK SYSTEMS, by Duane T. McRuer. July 1961. 71 p. incl. illus. (Proj. 8219; Task 82162) (ASD TR 61-118) Unclassified Report

A summary is given of techniques and concepts useful in the analysis of linear feedback systems; these procedures are then correlated and integrated into a unified analysis method. The central feedback system analysis problem discussed is that of finding complete closed-loop system characteristics from a knowledge of the open-loop transfer function. Several forms of graphical

(over)

UNCLASSIFIED

representation for open-loop transfer functions, including pole-zero plots and generalized G(s) logarithmic diagrams, are considered. The use of these graphical forms in generalized root-locus and decomposition techniques to find closed-loop transfer functions is illustrated with examples. The various feedback system analysis procedures are shown to have a common theoretical connection and to be supplementary techniques when used in an integrated manner to attack specific problems.

UNCLASSIFIED

Flight Control Laboratory, Aeronautical Systems Division, W-P Air Force Base, Ohio.

UNIFIED ANALYSIS OF LINEAR FEEDBACK SYSTEMS, by Duane T. McRuer. July 1961, 71 p. incl. illus. (Proj. 8219; Task 82162) (ASD TR 61-118) Unclassified Report

A summary is given of techniques and concepts useful in the analysis of linear feedback systems; these procedures are then correlated and integrated into a unified analysis method. The central feedback system analysis problem discussed is that of finding complete closed-loop system characteristics from a knowledge of the open-loop transfer function. Several forms of graphical

(over)

UNCLASSIFIED

representation for open-loop transfer functions, including pole-zero plots and generalized G(s) logarithmic diagrams, are considered. The use of these graphical forms in generalized root-locus and decomposition techniques to find closed-loop transfer functions is illustrated with examples. The various feedback system analysis procedures are shown to have a common theoretical connection and to be supplementary techniques when used in an integrated manner to attack specific problems.

UNCLASSIFIED

Flight Control Laboratory, Aeronautical Systems Division, W-P Air Force Base, Ohio.

UNIFIED ANALYSIS OF LINEAR FEEDBACK SYSTEMS, by Duane T. McRuer. July 1961, 71 p. incl. illus. (Proj. 8219; Task 82162) (ASD TR 61-118) Unclassified Report

A summary is given of techniques and concepts useful in the analysis of linear feedback systems; these procedures are then correlated and integrated into a unified analysis method. The central feedback system analysis problem discussed is that of finding complete closed-loop system characteristics from a knowledge of the open-loop transfer function. Several forms of graphical

(over)

UNCLASSIFIED

representation for open-loop transfer functions, including pole-zero plots and generalized G(s) logarithmic diagrams, are considered. The use of these graphical forms in generalized root-locus and decomposition techniques to find closed-loop transfer functions is illustrated with examples. The various feedback system analysis procedures are shown to have a common theoretical connection and to be supplementary techniques when used in an integrated manner to attack specific problems.

UNCLASSIFIED